OXIDATIVE DISSOLUTION OF BIO-U(IV)$O_{2(S)}$ IN PRESENCE OF NITRATE AND IRON UNDER ANAEROBIC CONDITIONS USING FLOW-THROUGH COLUMNS

A thesis submitted to graduate division of University of California Merced
in partial fulfillment of the requirements for the degree of

MASTERS OF SCIENCE

by

Rasesh Pokharel

August 16, 2013

I certify that I have read this dissertation and that, in my opinion, it is fully adequate in scope and quality as a thesis for the degree of Master of Science.

Dr. Peggy A. O'Day, Chair

I certify that I have read this dissertation and that, in my opinion, it is fully adequate in scope and quality as a thesis for the degree of Master of Science.

Dr. Samuel J. Traina

I certify that I have read this dissertation and that, in my opinion, it is fully adequate in scope and quality as a thesis for the degree of Master of Science.

Dr. Martha H. Conklin

ABSTRACT

This study investigates possible geochemical interactions between microbial reduced U(IV) species (Bio-U(IV)$O_{2(s)}$) and abiotic and biotic factors (Chemolithoautotrophic bacteria) affecting the stability of U(IV)-oxide minerals in anaerobic aquifers. Microbially mediated precipitation of Bio-U(IV)$O_{2(s)}$ produced a mixture of a U(IV) solid, mineral uraninite (UO_2(s)) and trace amounts of U(VI). Flow-through column experiments were performed to quantify biotic or abiotic oxidation of Bio-U(IV)$O_{2(s)}$, along with spectroscopic and microscopic techniques to characterize reactants and products. Results from flow through column experiments showed that release of U under anaerobic conditions is higher in presence of oxidants (NO_3^-, NO_2^-, Fe(III)) than with no oxidants. The presence of *Thiobacillus denitrificans* enhanced U release in the presence of 1 mM NO_3^-. However, in the system in which 5 mM soluble Fe^{2+} and 5 mM NO_3^- were present the release was significantly suppressed. One possible explanation is that *Thiobacillus denitrificans* favors oxidation of soluble Fe^{2+} over Bio-U(IV)$O_{2(s)}$. Soluble Fe^{2+} might form insoluble ferric oxide solids that sorb oxidized products of Bio-U(IV)$O_{2(s)}$. Spectroscopic data provided evidence of U(VI) in reacted columns in which Fe(II) was passed. These findings suggest that the presence or addition of another electron donor such as soluble Fe^{2+} in the field might suppress re-oxidation of uranium into soluble products that are released in aquifers.

ACKNOWLEDGMENTS

I would like to thank my M.S. advisory committee chair Dr. Peggy A O'Day, for her guidance and support throughout the last two years. Her excitement for science is contagious and kept me motivated during difficult times. Dr. Martha H. Conklin and Dr. Samuel J. Traina for their time and input during the final stages of this project. I would also like to thank Maria P. Asta who assisted with many analysis and offered valuable advice regarding experimental designs. My acknowledgements to Dr. Harry R. Beller and Peng Zhou from UC Berkeley lab for their support on the project. Masakazu Kanematsu and Nicolas Perdrial for their immense help during beamtime in SSRL. Also thanks to EAL director Liying Zhao for her effort and help during the sample run with ICP-MS. I am grateful to UC Merced group: Molly, Estela, Jeff and Chi-Shuo for their valuable effort with chemical analysis. I would also like to thank the US Department of Energy for their financial support. Finally, thanks to my family for what they have given to me.

TABLE OF CONTENTS

LIST OF FIGURES

LIST OF TABLES

1. INTRODUCTION

Reductive immobilization of uranium from contaminated sites using microbiology has been an efficient remediation strategy (Charbonneau, 2009). Uranium in its reduced form occurs as the mineral uraninite (UO_2) (s) or other reduced forms, which is insoluble, whereas in its oxidized state it occurs as the uranyl ion $(UO_2)^{2+}$, which forms water-soluble complexes (Langmuir, 1978). The main objective of many remediation strategies to remove uranium contamination from water is to convert it into its reduced state and make it insoluble. Many different types of dissimilatory metal (DMRB) and sulphate reducing bacteria (SRB), including *Shewanella*, *Geobacter* and *Desulfovibrio* species, couple the oxidation of organic matter and H_2 to the reduction of U(VI), resulting in U(IV) and the subsequent precipitation of uraninite (UO_2) or other U(IV) species other than uraninite (i.e. U(IV) monomeric species) (Lovley and Phillips, 1992a, b; Lovley et al., 1991; Lovley et al., 1993). Bioremediation strategy would be successful if the U(IV) formed remains stable or dissolution is slow enough so that the U(VI) formed is below the EPA drinking water threshold of 30 μg/L (EPA, 2000; Ulrich et al., 2008). However several studies have shown that the uranium U(IV) is not stable under some conditions and in time may oxidize to the soluble state.

Studies by Senko et al. (2002) and Beller (2005) showed that the oxidative dissolution of uraninite in a natural system should be a net effect of both biotic and abiotic processes. One major factor that contributes to the oxidation of uranium is the presence of nitrate, which can occur as a co-contaminant with uranium. Beller (2005)

showed that the bacterium *Thiobacillus denitrificans* is capable of anaerobic, nitrate-dependent oxidative dissolution of uraninite. Also iron is not a rare commodity in anaerobic environment, so it is important to understand the importance of its presence (Loveley and Lonergan, 1990). The ability of Fe^{3+} (hydr)oxides to oxidize both biogenic and abiogenic UO_2(s) to aqueous uranyl (UO_2^{2+}) is well known (Finneran et al., 2002; Ginder-Vogel et al., 2006; Sani et al., 2005b; Senko et al., 2007; Senko et al., 2005a; Senko et al., 2005b; Tokunaga et al., 2008; Wan et al., 2005). Presence of Fe^{2+} has been reported to decrease U(VI) release in batch experiments conducted by Sani et al. (2005a).

Therefore the roles of uranium, microbes, nitrate and iron are important to understand the dissolution and mobilization of uranium in anaerobic aquifers. There may be a variety of molecular-scale mechanisms such as precipitation reactions, dissolution reactions, adsorption reactions, and formation of aqueous complexes in the system that will determine the overall rate of dissolution. Factors such as the activities of aqueous species, pH, Eh, temperature, surface area of solids, and ionic strength of the system also play an important role. In order to understand the geochemical processes in the system, it is important to quantify these geochemical parameters.

The main objective of the project was to elucidate the key biotic and abiotic mechanisms underlying geochemical processes of anaerobic U(IV) and Fe(II) oxidation in the presence of NO_3^- and NO_2^-. Also the role of NO_3^- and NO_2^- species for U(IV) oxidation in presence of both ferrihydrite and soluble Fe^{2+} is studied. *Thiobacillus denitrificans* was used as biotic catalyst to understand enzymatic U(IV) and Fe(II) oxidation as well as microbial nitrate and nitrite reduction. In order to differentiate between rates of U(IV) oxidation by abiotic and biotic pathways, parts of the system were

isolated to determine overall rates of specific reactions. Flow-through column experiments were used to understand the dissolution process. Solids used in the column experiments were characterized by spectroscopic techniques in order to account for structural changes of uranium before and after the oxidation process.

2. METHODOLOGY

2.1 Quartz cleaning

Trace metal impurities from quartz were removed by heating at 450 ^{o}C for 48 h. After heating, quartz was refluxed in 4 N HCL at 65 ^{o}C for 4 h. The quartz was cleaned with 0.1 M NaCl solution by centrifuging for 6 min at 3300 g 21 times. The supernatant was decanted, the solid was rinsed in 2 N NaOH for 2 h, centrifuged, neutralized with HCl, and rinsed with 18.2 MΩ cm^{-1} water several times. Finally the quartz was dried at 65^{o}C for 24 h.

2.2 Ferrihydrite coating on quartz

Synthetic 2-line ferrihydrite solution was prepared by modifying the method described by Cornell and Schwertmann (1996). 175 mL of 0.06 M $FeCl_3 \cdot 6\ H_2O$ was titrated with 1 M NaOH to pH 7 while vigorously stirring. The pH of the solution was maintained for at least 2 h. The solution was then centrifuged three times at 3300 g at 20^{o}C for 5 min using 18.2 MΩ cm^{-1} water. Excess liquid was decanted and the resulting ferrihydrite precipitate was mixed with 50 g of pre-cleaned quartz. The mixture of ferrihydrite and quartz was again washed with 18.2 MΩ cm^{-1} water by centrifuging at

3300 g for 5 min at 20^{o}C three times. The resulting ferrihydrite and quartz mixture was stirred, purged with N_2 gas and dried at room temperature for three days while periodically stirring. The dried mixture was then flushed with 18.2 MΩ cm^{-1} water five times and again dried at room temperature for three more days. The ferrihydrite-coated quartz was stored at 4^{o}C. The amount of Fe coated on quartz was determined by dissolution of ferrihydrite with 2 M HCl at 80^{o}C for 12 h, followed by quantification of Fe by spectrophotometry. Spectrophotometric results showed that about 2 mg of Fe was coated on 1 g of quartz.

2.3 Biogenic U(IV)-oxide synthesis

Reduced uranium solid (referred to here as Bio-U(IV)$O_{2(s)}$) was synthesized by microbial reduction following Schofield et al. (2008) and (Veeramani et al., 2009). Aqueous uranyl (UO_2^{2+}) was reduced using *Shawenella oneidensis* strain MR-1 at pH 6.3. Fresh colonies of *S. oneidensis* were grown in 1 L of Luria-Bertani (LB) media under ambient room conditions. The cell suspension was then centrifuged at 10,000 g for 12 min to separate the cells from the LB media. The separated cells were centrifuged and washed 3 times at 10,000 g for 12 min with a medium containing 30 mM $NaHCO_3$, 20 mM PIPES and 20 mM lactate (pH adjusted to 6.3) under anaerobic conditions (10% H_2, 90% Ar). The cells were re-suspended in the same solution and adjusted to an optical density (OD_{600}) of one. Then 1500 μM of uranyl acetate solution was added and the solution was kept under anaerobic conditions for four days for the U to reduce and precipitate. The reduced U(IV) solid was recovered by centrifugation (which caused formation of a solid pellet) and then re-suspended in 1 M NaOH for 12 h. The solid was

centrifuged again and re-suspended in hexane (previously made anoxic by vacuuming and gassing three times with Ar) for another 12 h. Finally the solid was centrifuged and stored in a 1 M $NaHCO_3$ solution under anaerobic conditions. Three different batches of Bio-U(IV)$O_{2(s)}$ synthesis (labeled as Unr-1, Unr-2 and Unr-3) was done in the project. Various different analysis (BET, SEM, TEM, XRD, DLS, EXAFS) were done for Unr-1 and Unr-2. Detail information about each characterization is discussed in Analytical Methods (Section 3). Table 1 provides information about various analyses performed for the Unr-1 and Unr-2 solids.

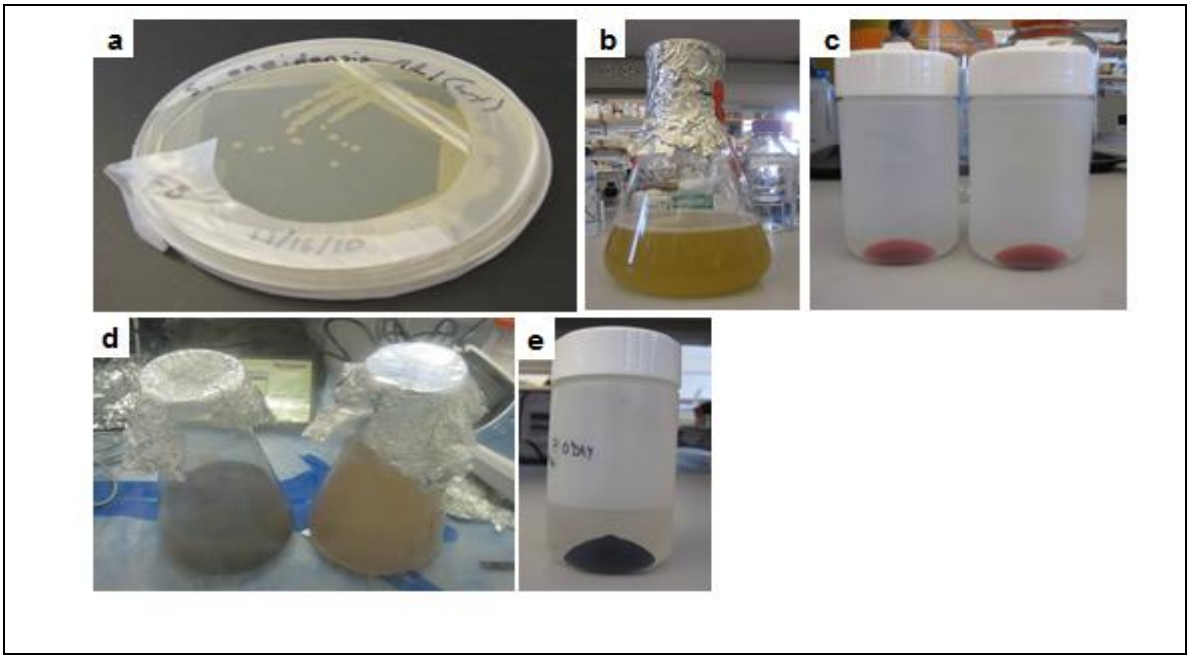

Figure 1. Bio-U(IV)$O_{2(s)}$ synthesis by *Shewanella Oneidensis* strain MR-1: (a) *S. Oneidensis* strain MR-1; (b) liquid culture (LB, aerobic conditions); (c) pellets of *S. Oneidensis*; (d) anaerobic phase uranyl acetate + PIPES + $NaHCO_3$ + Na-Lactate solution; (e) Bio-U(IV)$O_{2(s)}$.

Table 1. Characterizations of various batches of unreacted Bio-U(IV)$O_{2(s)}$

Bio-U(IV)$O_{2(s)}$ Sample ID	Characterizations				
	XRD	BET	DLS	TEM	EXAFS
Unr-1	✔	✔		✔	✔
Unr-2			✔	✔	✔
Unr-3					

"Unr" refers as unreacted. Detail information of how these characterizations were done is provided on the Analytical Methods section.

2.4 *Thiobacillus Denitrificans* cultivation and incubation

Thiobacillus denitrificans (strain ATCC 25259) was cultured in an anaerobic pH 7 nutrient medium by following the procedure described in Beller (2005). The media was specifically designed for cultivation of *Thiobacillus denitrificans*. The medium consisted of following compounds added at the indicated concentrations in 1 L of 18.2 MΩ cm^{-1} water: $Na_2S_2O_3 \cdot 5H_2O$ (20 mM), NH_4Cl (18.7 mM), KNO_3 (20 mM), KH_2PO_4 (14.7 mM), $MgSO_4 \cdot 7H_2O$ (3.25 mM), $FeSO_4 \cdot 7H_2O$ (0.08 mM). Then the media was made sterile by autoclaving for 30 min at 121^o C. The media was allowed to cool for some time till it was warm. Then anaerobic and sterile sodium bicarbonate solution, calcium chloride solution along with vitamin, trace element and selenate-tungstate solutions which correspond to the stock solutions 1, 4, 6, 7 and 8 as described by Widdel and Bak (1992) was added in the warm media using sterile syringes. Then 10 mL of the media was transferred in an anaerobic sterile sealed culture tube and *Thiobacillus denitrificans* (strain ATCC 25259) was also added. The cultures were allowed to grow 30^o C under anaerobic conditions without shaking until the absorbance was between 0.07 - 1.5. Then 5 mL of the culture tube was mixed with 200 mL of the media on a 250 mL centrifugable

bottle which was kept under anaerobic conditions. The culture in the centrifuge bottles was grown for another 48 h at 30^{o} C without shaking. Immediately before the start of column experiments, the culture was harvested by centrifugation at 9300 g for 30 min, washed, and resuspended in a sterile saline solution.

2.5 Anaerobic flow-through column experiment

Experiments were done in anaerobic conditions at room temperature (25±1ºC) in a Coy anaerobic glove box (Type A Vinyl Anaerobic Chamber) with a gas mixture of 90 % N_2 and 10 % H_2. Partial pressure of oxygen was continuously monitored using a gas analyzer (Model 10, Coy Laboratory Products Inc). One liter of deionized water (18.2 MΩ. cm^{-1}) used for all solutions was boiled for 30 min to remove dissolved oxygen. All the equipment, reagents, and solutions were placed in the glovebox at least 24 h before the experiment.

2.5.1 Abiotic experiments

The columns used for abiotic experiments were polypropylene chromatography columns (SUPELCO; volume: 1 mL; length: 2 cm). Influent solutions prepared in the glovebox were filtered with a 0.2 µm polycarbonate filter (Millipore sterile filters) at both the inlet and outlet ends of the column. Tubing (2-Stop PharMed BPT) was used to connect the columns to the input solution reservoir and the fraction collector for the effluent solution. Flow rates of 0.025- 0.028 mL/min were maintained using a HPCL pump (Ismatec model, C.P. 78001-02). Flow was directed upwards in the columns to minimize N_2 gas pressure. An ORION 081010MD electrode was used to continously

measure dissolved oxygen in the input solutions. A Thermo Scientific Orion 9102DJWP pH electrode was used to set or periodically measure the input solution pH. A known mass of Bio-U(IV)$O_{2(s)}$ and ferrihydrite-coated quartz was weighed separately. The solids were then mixed by hand and packed into the column in small amounts using constant pressure to obtain good compaction. Columns were weighed before and after packing. Input solutions used for both abiotic and biotic experiments were prepared by mixing respective analytical reagents (NO_3^-, NO_2^-, Fe^{2+}, NaCl or MOPS) with pH adjusted to 6.9-7.0 using 2 M NaOH. Table 2 provides detail of each experimental setup. The effluent solution was collected at about 5.5 mL increments with a fraction collector (Spectra/Chrom® CF-1). pH and Eh were not measured in the effluent solutions. After the experiment was completed, solid samples from the columns were immediately separated into different aliquots for different characterizations and stored at -80ºC.

Table 2. Experimental conditions and parameters for abiotic experiments

Column[1]	Input solution reagents				Pore volume / days	Bio-U(IV)$O_{2(s)}$ batch	Flow rate[2] (mL/min)	Initial U mass[3] (mg)	Tot U in reacted columns[4] (mg)	Initial Fe mass[5] (mg)
	NO_3^- mM	NO_2^- mM	NaCl mM	Fe^{2+} mM						
AB-1			10		498/4	Bio-Unr-3	0.028	1.85±0.05	1.63±0.07	4.08
AB-2		1	9		498/4	Bio-Unr-3	0.028	1.33±0.09	1.02±0.08	0
AB-3-a		1	9		498/4	Bio-Unr-3	0.028	1.85±0.05	1.51±0.08	4.08
AB-3-b		1	9		498/4	Bio-Unr-3	0.028	1.86±0.05	0.463±0.03	4.1
AB-5			5	5	498/4	Bio-Unr-2	0.028	1.71±0.06	1.36±0.44	NM
AB-6	5			5	498/4	Bio-Unr-2	0.028	8.35±0.06	1.43±0.04	0
AB-7	5		5		498/4	Bio-Unr-2	0.028	1.71±0.06	1.49±0.47	NM
AB-8	5			5	498/4	Bio-Unr-2	0.028	1.71±0.06	1.43±0.11	NM

[1] Columns used in the experiments were 1 mL column. [2] Flow rate was calculated by measuring the amount of effluent solution with time. [3] Initial mass of Bio-U(IV)$O_{2(s)}$ packed in the columns, values obtained from microwave digestion followed by ICP-MS analysis. [4] Mass of total U remaining at the end of experiment, values obtained from microwave digestion followed by ICP-MS analysis. [5] Initial mass of Fe packed in column, values obtained from microwave digestion followed by ICP-OES analysis. All the input solutions were adjusted to pH 6.95 ± 0.05 using MOPS buffer. Bio-U(IV)$O_{2(s)}$ was mixed with ferrihydrite-coated quartz except in columns AB-2 and AB-6 where quartz was used. NM is not measured.

2.5.2 Biotic experiments

The experimental procedure for biotic experiments was similar to the abiotic experiments described above. However, 6 mL polypropylene chromatography columns (SUPELCO) (length: 4.5 cm) were used and thus, a larger mass of Bio-U(IV)$O_{2(s)}$ (≈ 40 mg) and ferrihydrite-coated quartz (8.5 g) was packed into the column. The re-suspended *Thiobacillus denitrificans* cells were diluted with the buffer solution (MOPS and NaCl, pH 7.2) until the OD of 2 was achieved. Then 1 mL of the cell solution was added in the mixture of quartz and biogenic uraninite, and was packed into the column. Table 3 provides detail of each experimental setup of the biotic experiments.

Table 3. Experimental conditions and parameters for biotic experiments

Column[1]	Input solution reagents			*T. denitrificans* (OD)[6]	Pore volume / days	Bio-U(IV)$O_{2(s)}$ batch	Flow rate[2] (ml/min)	Initial U mass[3] (mg)	Final U mass[4] (mg)	Initial Fe mass[5] (mg)
	NO_3^- mM	NaCl mM	Fe^{2+} mM							
Bio-1-CNT	1	9			200 / 4	Bio-Unr-1	0.070	2.29±0.29	2.87±0.11	17.84
Bio-1-a	1	9		2	200 / 4	Bio-Unr-1	0.070	2.31±0.30	6.46±0.39	17.94
Bio-1-b	1	9		2	200 / 4	Bio-Unr-1	0.070	2.32±0.30	2.76±0.09	18.04
Bio-1-c	1	9		2	200 / 4	Bio-Unr-1	0.070	2.29±0.29	2.62±0.09	17.79
Bio-2-CNT	5		5		300 / 7	Bio-Unr-2	0.060	10.47±0.50	NM	NM
Bio-2-a	5		5	1	300 / 7	Bio-Unr-2	0.060	10.53±0.51	3.51±0.35	NM
Bio-2-b	5		5	1	300 / 7	Bio-Unr-2	0.060	10.44±0.51	16.35±1.3	NM
Bio-2-QTZ	5		5	1	300 / 7	Bio-Unr-2	0.060	3.5±0.21	3.72±0.15	NM

[1] Columns used in the experiments were 6 mL column. [2] Flow rate was calculated by measuring the amount of effluent solution with time. [3] Initial mass of Bio-U(IV)$O_{2(s)}$ packed in the columns, values obtained from microwave digestion followed by ICP-MS analysis. [4] Mass of total U remaining at the end of experiment, values obtained from microwave digestion followed by ICP-MS analysis. [5] Initial mass of Fe packed in column, values obtained from microwave digestion followed by ICP-OES analysis. [6] OD: Optical density, which was the absorbance of *T. denitrificans* measured by spectrophotometry at 600. All the input solutions were adjusted to pH 6.95 ± 0.05 using MOPS buffer. Bio-U(IV)$O_{2(s)}$ was mixed with ferrihydrite-coated quartz except in columns Bio-2-QTZ where quartz was used. NM is not measured.

A bromide tracer was used to determine column transport properties. Tracer tests were performed in both biotic and abiotic columns using an Envco BR43-0001 electrode. The electrode has an detection limit of 0.4 ppm Br^-. Bromide tracers were performed on experimental flowrates at 40 ppm Br^- ±2% error. Figure 2 shows a schematic diagram of experimental planning and types of biotic and abiotic experiments performed in the research.

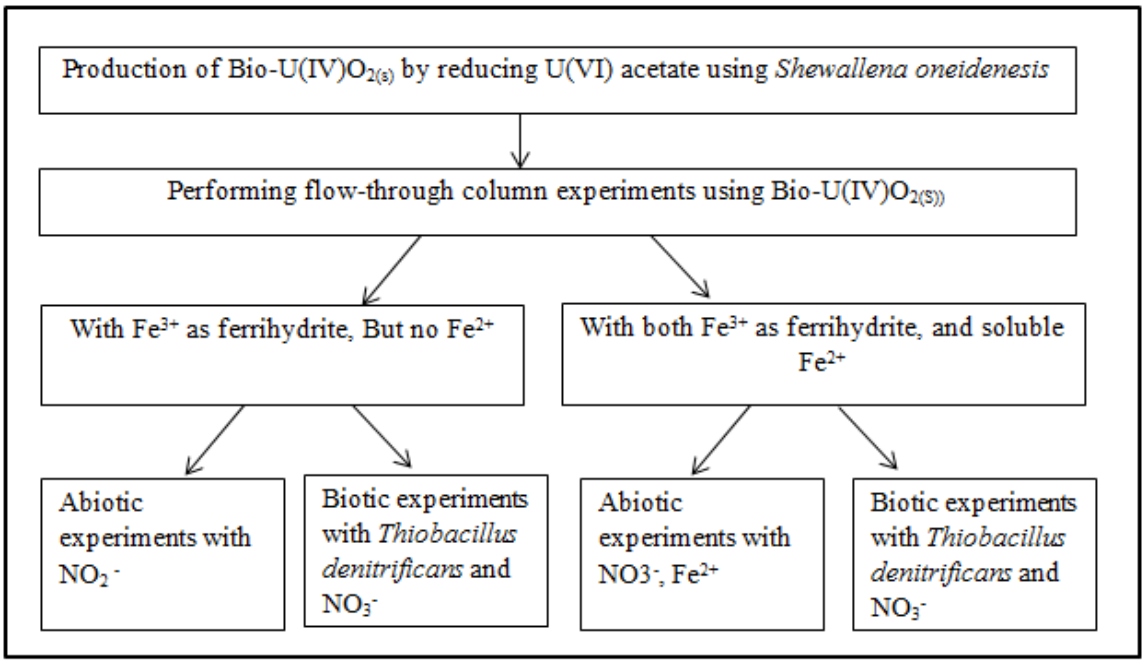

Figure 2: Schematic of overall experimental planning

3. ANALYTICAL METHODS

All the chemical reagents used for analytical purposes were a purity at least equal to the reagent-grade standards of the American Chemical Society.

3.1 ICP-MS analysis (U and Fe)

Column effluent solutions were analyzed for total uranium by inductively coupled plasma mass spectrophotometry (ICP-MS, Agilent 7500cs). Variable sample dilutions from 1:2 to 1:5 were done using an Optima grade 2% HNO_3. Detection limits for uranium and iron were 4.2×10^{-5} µmol/L (10 ppt), and analytical precision was < 5%. Linear response was measured by calibration standards over four orders of magnitude ($R > 0.999$). Accuracy of the instrument was confirmed by checking blanks and standards after every 12 samples.

3.2 Spectrophotometeric analysis

Nitrate, nitrite , iron(II) and total iron (also referred to here as NO_3^-, NO_2^-, Fe^{2+} and Fe^{tot} respectively) concentrations were determined spectrophotometrically with a 4 cm (NO_3^- and NO_2^-) and 1 cm (Fe^{2+} and Fe^{tot}) light path cell in a Cary-300-Bio spectrophotometer, discussed below.

3.2.1 Nitrite

Nitrite analysis was done following the procedure by Bendschneider and Robinson (1952). Two types of reagent, sulfanilamide (SAN) reagent and N-1-napthylenediamine dihydrochloride (NED) reagent, were used. The SAN reagent was prepared by adding 10 g SAN to 1 L of 1.2 N hydrochloric acid and the NED reagent by adding 1 g of NED to 1 L 18.2 MΩ cm^{-1} water. Samples and standards were diluted up to 10 mL with 18.2 MΩ cm^{-1} water over a concentration range from 0.2 to 4.5 µmol/L. Sulfanilamide reagent (0.2 mL) was added to the diluted sample and allowed to react for 2 to 8 min. Next, 0.2 mL of NED reagent was added and immediately mixed. Samples

were allowed to stand for 10 min and were measured immediately at 543 nm wavelength. Detection limit of the instrument was found to be 0.1 µmol/L for NO_2^- measurements.

3.2.2 Nitrate

Nitrate was analyzed following the protocol described in Goldman and Jacobs (1961). Volume of 10 mL of sample or standard was prepared by diluting appropriate amounts with 1% HCl. Absorbance were measured at 220 nm wavelength. Detection limit of the instrument was found to be 1.6 µmol/L for NO_3^- measurements.

3.2.3 Iron (II) and total iron

Iron (II) and total iron analysis were performed by modifying the ferrozine analysis method of Viollier et al. (2000). Three types of reagents were required for the analysis:

Reagent I: 0.01 M Ferrozine prepared in a 0.1 M ammonium-acetate (CH_3COONH_4).

Reagent II: 1.4 M Hydroxylamine hydrochloride ($NH_2OH.HCl$) prepared in 2 M hydrochloric acid (reducing reagent for total iron analysis).

Reagent III: 5 M ammonium acetate buffer adjusted to pH 9.5 M using ammonium hydroxide (28-30 % NH_4OH).

For Fe^{2+} analysis, 1 mL of the sample or standard diluted with 0.1 M HCl was mixed with 100 µL of reagent I. The solution was allowed to stand for 10 min and then 50 µL of reagent III was added. For Fe^{tot} analysis, 1 mL of sample or standard was mixed with 100 µl of reagent I and then 150 µL of reagent II was added. The mixture was allowed to stand for 10 minutes and then 50 µL of reagent III was added. Sample

absorbance for both analyses was measured at 543 nm. Detection limit of the instrument was found to be 1 µmol/L for Fe^{2+} and Fe^{tot} measurements.

3.3 Solid Analysis:

3.3.1 Acid digestion and ICP-MS

Reacted and unreacted samples from the column (0.5 -1 g) were dried in an oven at 105^{o} C overnight to calculate water content. The dried samples were digested in 3 mL concentrated HNO_3 and 9 mL concentrated HCl by microwave digestion (165^{o} C, 200 atm) in teflon vessels. Acid solutions were filtered using a 0.45 µm filter syringes, diluted, and total U, Fe concentrations were measured by ICP-MS.

3.3.2 XRD

X-ray diffraction (XRD) data for Bio-U(IV)$O_{2(s)}$, crystalline $UO_{2(s)}$ (International Bio-Analytical Industries, Inc. CAS# 1344-57-6) and ferrihydrite were collected on a PANalytical X'pert Pro diffractometer with an ultra-fast X'Celerator detector. All the samples were mounted on a zero background Si holders. For Bio-U(IV)$O_{2(s)}$ analysis, samples were mounted on the Si holders and maintained under anaerobic conditions until analysis. For crystalline $UO_{2(s)}$ analysis, about 0.5 g of samples was placed in 3 mL of 1 N HNO_3 acid for 2 hours inside the glovebox to remove any salt precipitates in the surface. Then the samples were dried overnight, hand grinded using mortar and pestle and were mounted on the Si holders. Samples of Bio-U(IV)$O_{2(s)}$ and crystalline $UO_{2(s)}$ were scanned from 4 to 75 degree 2θ with 0.008 step size with a Co Kα source. Ferrihydrite sample preparation was done by mounting freshly prepared ferrihydrite

precipitate on the zero background Si holders. Samples were scanned from 25 to 90 degree 2θ step size of 0.008 with a Co Kα source.

3.3.2 SEM and TEM

Scanning electron microscope (SEM) and transmission electron microscope (TEM) techniques were used for ultrastructure examinations of unreacted Bio-U(IV)$O_{2(s)}$. Bio-U(IV)$O_{2(s)}$ samples were suspended in methanol and sonicated for 24 h. Then 10 µL of the suspension were mounted on Al-alloy stub mounts with double-stick carbon tape (for SEM) and Cu grids (for TEM). The samples were dried under anaerobic conditions. Samples were examined with a FEI Quanta 200 ESEM with tungsten filament and EDAX Genesis energy-dispersive X-ray spectrometer at 20 kV at a working distance of 5-10 mm and magnifications from 1700x to 10,000x were used for SEM analysis. TEM images were obtained by a JEOL-JEM-2010 HRTEM microscope operating at 200 kV.

3.3.3 BET surface area analysis

The surface areas of Bio-U(IV)$O_{2(s)}$ and ferrihydrite samples were obtained using the BET method. Micrometrics Tri-Star 3000 surface area analyzer was used for surface area measurements. Bio-U(IV)$O_{2(s)}$ samples were dried at 110 ^{o}C to remove water before the analysis. BET measurements for both Bio-U(IV)$O_{2(s)}$ and ferrihydrite were done using a ultra- high purity N_2 gas. Seven points were collected in the measurement and the isotherm was analyzed using software from Micrometrics.

3.3.4 DLS particle size analysis

Particle size analysis of unreacted Bio-U(IV)$O_{2(s)}$ sample was done by following Dynamic Light Scattering (also known as Photon Correlation Spectroscopy or Quasi-Elastic Light Scattering) technique using a Brookhaven Laser Spectrometer (Brookhaven Instruments, NY, USA). About 10 mg of Fresh Bio-U(IV)$O_{2(s)}$ sample were suspended in 3 mL of methanol and sonicated for 12 h. Sample vials used for the measurements were cleaned with 0.1 N HCl and filtered 18.2 MΩ cm^{-1} water. The suspended Bio-U(IV)$O_{2(s)}$ sample were directly poured in a clean vial and measured.

3.3.5 X-ray absorption spectroscopy (XAS) analysis

Uranium L_{III} X-ray absorption spectra of unreacted and reacted Bio-U(IV)$O_{2(s)}$ were collected at the Stanford Synchrotron Radiation Lightsource (SSRL) on beamline 4-1 and 11-2. Unreacted Bio-U(IV)$O_{2(s)}$ mixed with ferrihydrite-coated quartz, unreacted Bio-U(IV)$O_{2(s)}$ mixed with quartz, and reacted Bio-U(IV)$O_{2(s)}$ samples from the column experiments were ground using mortar and pestle inside an anaerobic glove box. The dilution factor of Bio-U(IV)$O_{2(s)}$ to quartz or ferrihydrite-coated quartz was close to 1:100 for all the samples. Samples were loaded within slots in an aluminum sample holder using Kapton tape. After loading, the samples were shipped to SSRL within two days in a hermetically sealed stainless steel anaerobic jar (Schuett-Biotec).

At beamline 4-1, U-L_{III} absorption spectra were collected using a Si(220) Phi = 90 double crystal monochromator calibrated with Y foil (first edge inflection set to 17038 eV) and a U standard (powdered UO_2(s)) (edge inflection at 17166 eV). Fluorescence L_{III} EXAFS spectra were collected using a 13-channel Ge fluorescence detector, 30%

detuned from maximum intensity to decrease harmonic and scattered radiation. Beam size was set to 1 mm vertical by 4 mm horizontal. During data collection, the samples were held in a liquid N_2-cooled cryostat. Up to 15 scans were collected in fluorescence mode to increase signal to noise. On beamline 11-2, UL_{III} spectra were collected using a Si(220) Phi = θ double crystal monochromator that was calibrated similarly to BL 4-1 using Y foil and U foil standard. However, BL 11-2 had a 100-element Ge detector, which provided better signal to noise with fewer scans compared with the detector on BL 4-1. Beam size was adjusted to 1 mm vertical by 4 mm horizontal and the beam was detuned 20% from maximum intensity. Samples were held in a liquid N_2-cooled cryostat similar to BL 4-1 and up to 8 scans were collected in fluorescence. EXAFS spectra were averaged using SIX-PACK (Webb, 2005), while Athena was used to background subtract, spline and analyze (Ravel and Newville, 2005). A linear fit through the pre-edge region and a spline fit through the EXAFS region with value of 17185 eV for K = 0 A^{-1} was done for background subtraction.

4. RESULTS

4.1 Particle size and surface area analysis

The hydrodynamic diameter of unreacted Bio-U(IV)$O_{2(s)}$ (Unr-2) solid particles (Bio-Unr-2) measured by DLS showed two prominent peaks around 50 nm and 500 nm (Figure. 3). These results indicate that the particle size in the Bio-U(IV)$O_{2(s)}$ sample was

not homogeneous and that particles tend to aggregate. The N_2-BET surface area of the unreacted sample (Unr-1) was 78.31 ± 0.56 m^2/g.

The N_2-BET surface area of freshly prepared ferrihydrite was high (343 ± 3 m^2/g), which is in the range of reported values in other studies (Moon and Peacock, 2013; Schwertmann and Cornell, 2007).

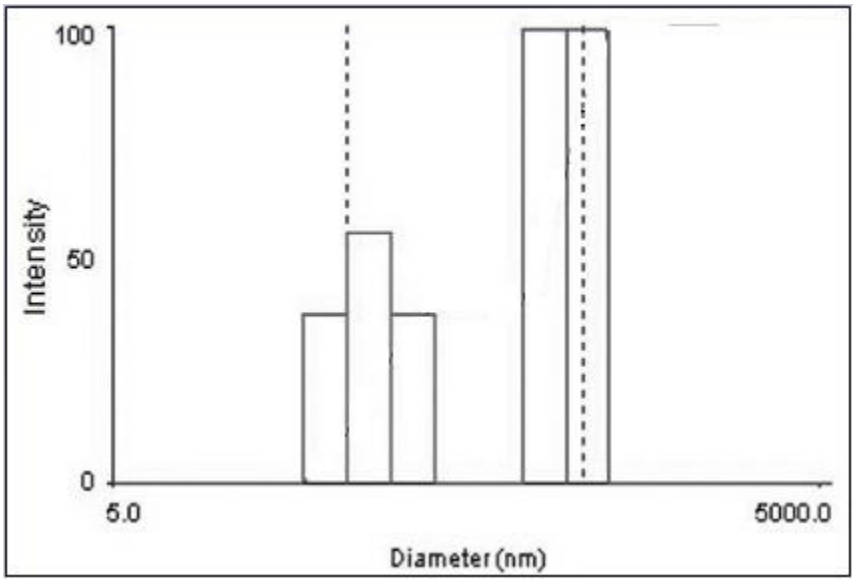

Figure 3: Particle size analysis of Bio-U(IV)$O_{2(s)}$ (Unr-2) using Dynamic Light Scattering technique. The graph shows high intensity of peaks at around 50 and 500 nm.

4.2 Electron microscopy

The SEM and TEM images of unreacted Bio-U(IV)$O_{2(s)}$ suggested that nanoparticles are heterogeneously distributed in the sample and tend to form aggregates. Figure 4 shows images of the morphology and particle size of Bio-U(IV)$O_{2(s)}$ observed by SEM and TEM, respectively. The SEM image showed that Bio-U(IV)$O_{2(s)}$ consist of rounded particles that form aggregates up to several microns in diameter. The lattice

fringes observed in the TEM images predict the particle size to be around 4 nm in size and rounded morphology.

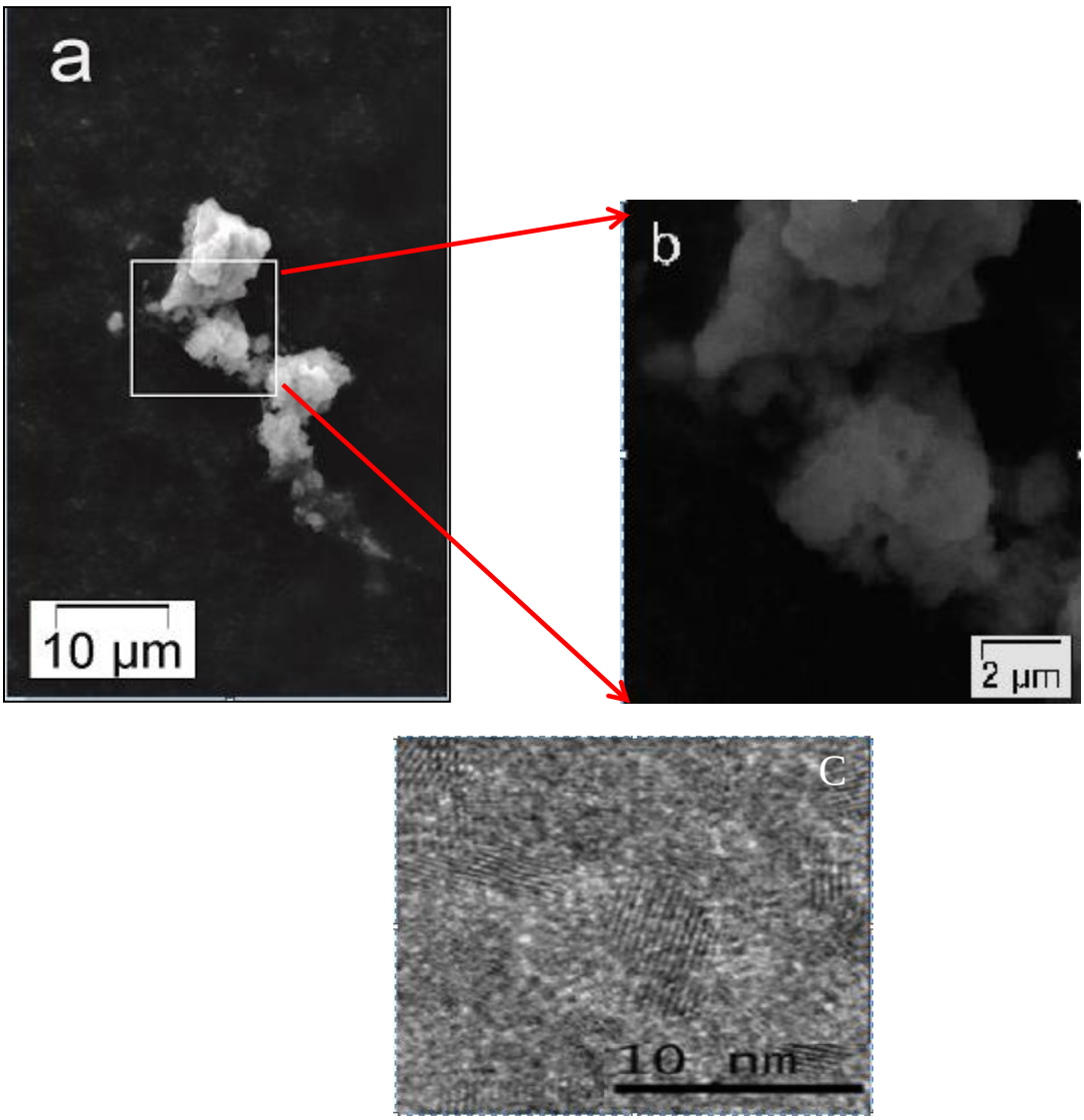

Figure 4. SEM (a,b) and TEM images (c) of Bio-U(IV)$O_{2(s)}$ (Unr-1) solid.

4.3 XRD analysis

The XRD pattern of synthetic crystalline UO_2(s) showed peaks at 32.94^0, 38.22^0, 55.12^0, 65.71^0 (2Θ degrees, Co K-α source). The diffractogram of unreacted Bio-

U(IV)$O_{2(s)}$ (Unr-1) showed peak positions similar to that of crystalline UO_2(s). However, peaks are short and broad, suggesting small particle and amorphous solids (Fredrickson et al., 2000; Waychunas, 2001).

The diffractogram of ferrihydrite showed two major reflections at 41^0, 74^0 (2Θ degrees), which is consistent with the result for 2-line ferrihydrite shown by Loan et al. (2005). The short and board nature of the peaks indicates the solid to be amorphous.

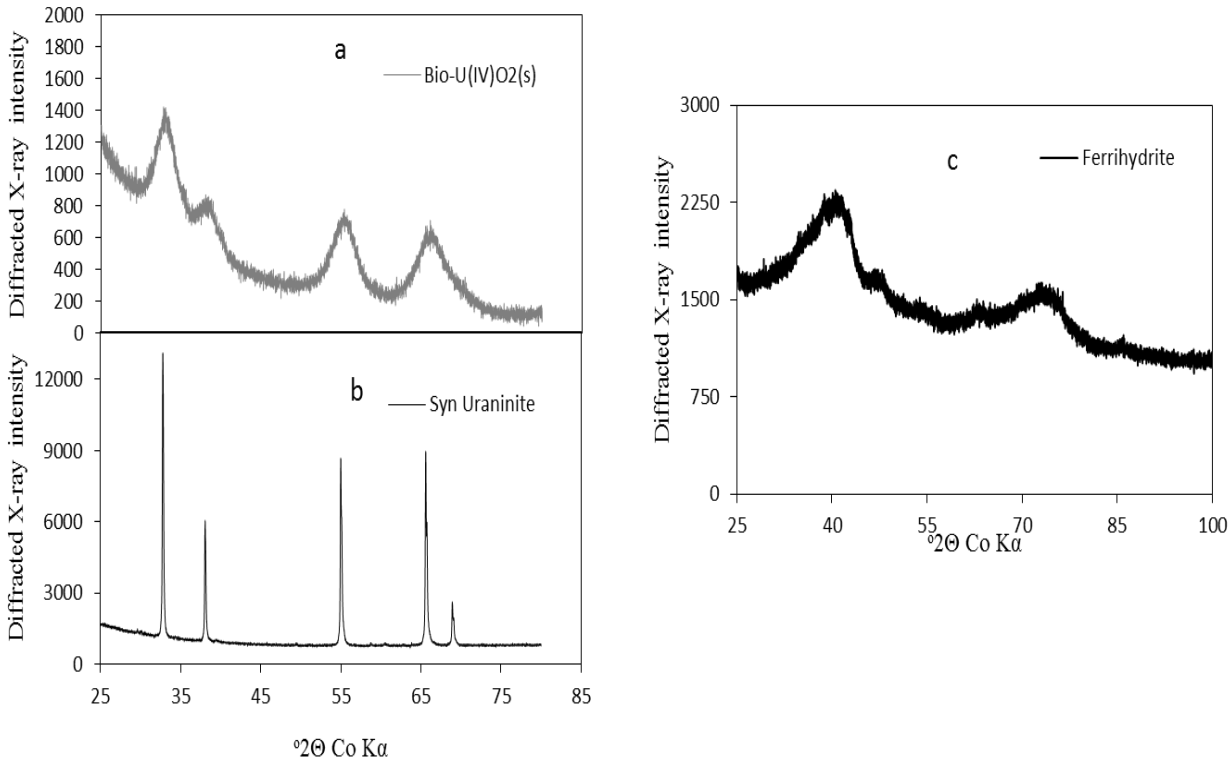

Figure 5. Powder XRD patterns of Bio-U(IV)$O_{2(s)}$ (Unr-1) (a) and synthetic uraninite ($UO_{2(s)}$) (b) and freshly prepared ferrihydrite (c).

4.4 XAFS analysis

Figure 6 shows comparison of EXAFS and Fourier transform spectra (FTs) to account for changes between reacted and unreacted samples. Unr-1 diluted with quartz

was used as a reference for unreacted Bio-U(IV)$O_{2(s)}$, whereas mineral schoepite ($(UO_2)_8O_2(OH)_{12}$•$12(H_2O)$) was used as U(VI) reference. Although a U-O shell at around 2.35 Å and a U-U at around 3.86 Å in the Unr-1 sample resembled stoichiometric $UO_{2(s)}$ spectra.

No significant changes was found in EXAFS and FTs between Unr-1 and Bio-1-a and Bio-1-CNT. Bio-1-a showed a slight increase in amplitude in the FT peak of the U-U shell in comparison to Unr-1 sample. The reasons for increase might be due to oxidation, but it is not properly understood. However smoothing of the curve from 6 Å to 8 Å in the EXAFS of reacted column in presence of Fe(II) (Bio-2-a, Bio-2-CNT and Bio-2-Qtz) resembles features similar to mineral schoepite (Figure. 6b1). This might indicate oxidation of Bio-U(IV)$O_{2(s)}$ to U(VI) in presence of Fe(II). Future work will be done to analyze the unreacted and reacted Bio-U(IV)$O_{2(s)}$. XANES analysis will be performed in order to account for oxidized U(VI) bound in the unreacted and reacted Bio-U(IV)$O_{2(s)}$. Also EXAFS fitting models will be used in order to understand the structural changes due to oxidation process.

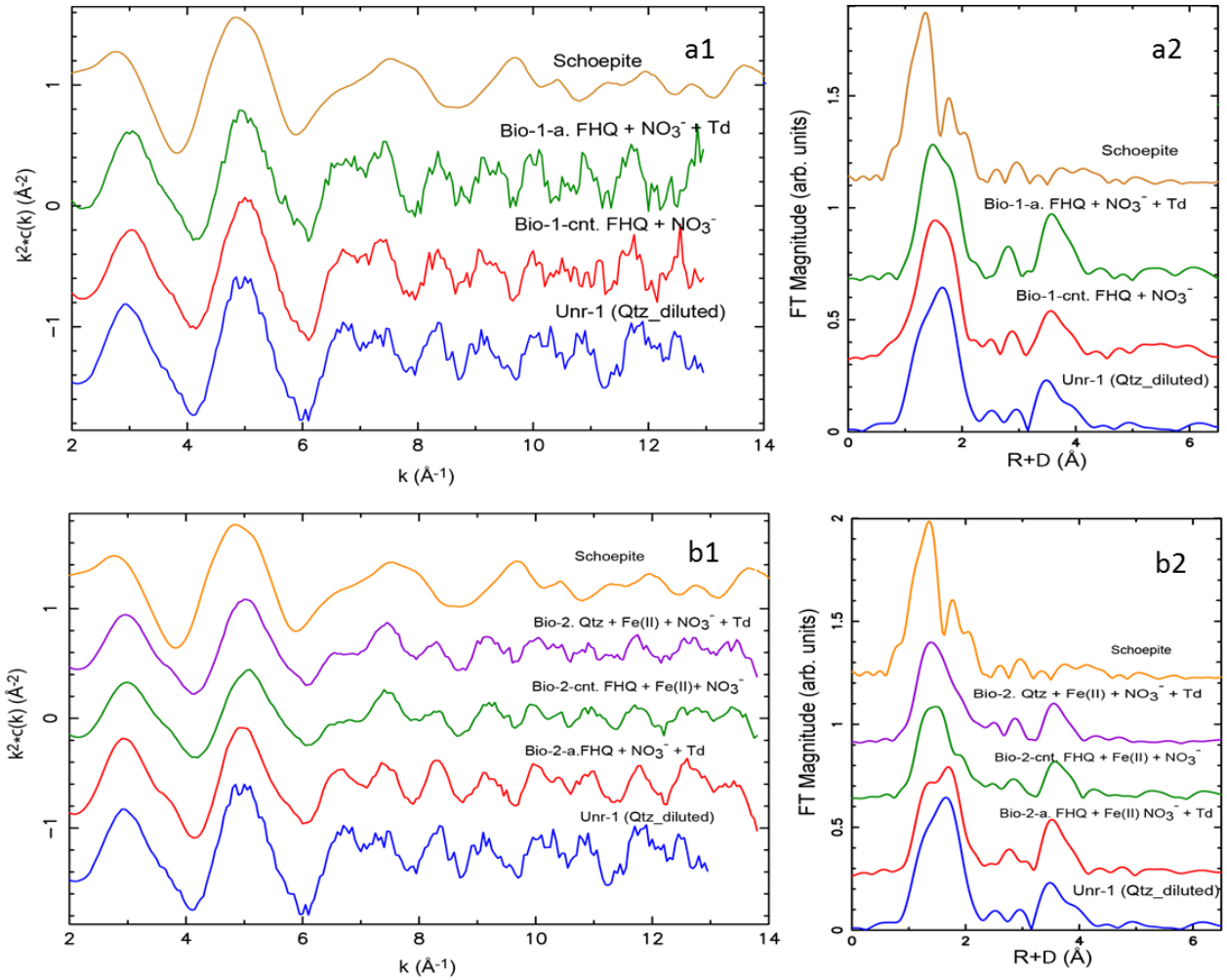

Figure 6: EXAFS and Fourier transform comparison between reacted and unreacted Bio-$U(IV)O_{2(s)}$. Unr-1 (Qtz_diluted) was used as an reference for unreacted Bio-$U(IV)O_{2(s)}$, whereas the mineral schoepite as the U(VI) reference.

4.5 Flow-through column experiments

4.5.1 Column hydrodynamic properties

The bromide tracer curve for one biotic and one abiotic column is shown in Figure 7. The biotic columns were 6 mL columns, whereas the abiotic columns were 1 mL in volume. The shape of rising limb of the curves is a function of dispersivity, whereas the time of arrival of peak concentration (40 ppm) is the effective porosity for both the columns.

Future work includes using CTXFIT to model the curve to get the difference in dispersivity between the biotic and abiotic columns.

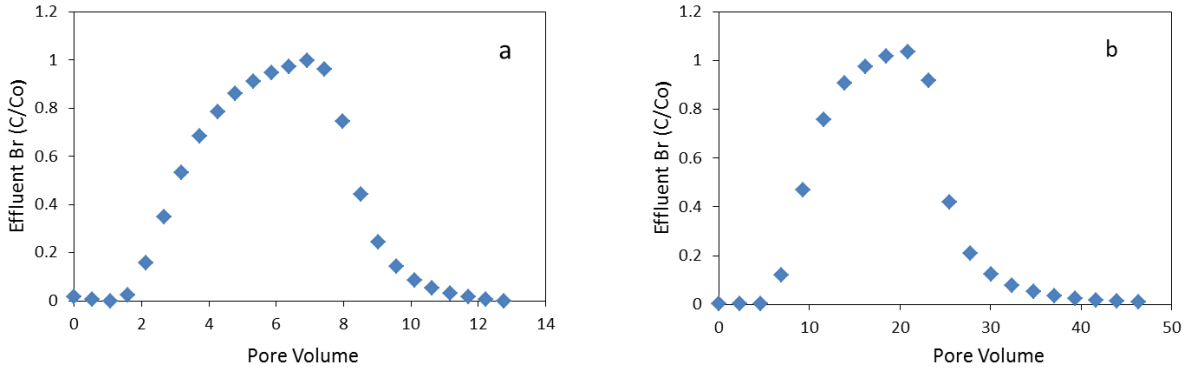

Figure 7. Representative effluent concentrations of the conservative Br- tracer shown as effluent concentration (C) divided by influent concentration (C_o) from reacted biotic column (a) and reacted abiotic column (b)

4.5.2 Biotic columns without Fe^{2+}

In presence of *T. denitrificans* and NO_3^- (Bio-1-a, Bio-1-b, Bio-1-c), U release was significantly higher than the abiotic control without *T. denitrificans* (Bio-1-CNT) (Figure. 8a). Uranium release was not observed for the first 100 pore volumes (PV) for the biotic columns, but U release increased significantly afterwards. However, steady state for U release was not obtained in the biotic experiments. Results showed that *T. denitrificans* stimulates U release, suggesting that the presence of the bacteria catalyzes Bio-U(IV)$O_{2(s)}$ oxidation. The amount of NO_2^- released in the presence of *T. denitrificans* had variations within the triplicates, with Bio-1-a and Bio-1-b releasing higher U concentrations but Bio-1-c releasing concentrations similar to the control (without *T. denitrificans*) (Figure. 8b). Effluent concentrations of NO_3^- were constant within the 10 % error range of spectrophotometric method (Figure 8c).

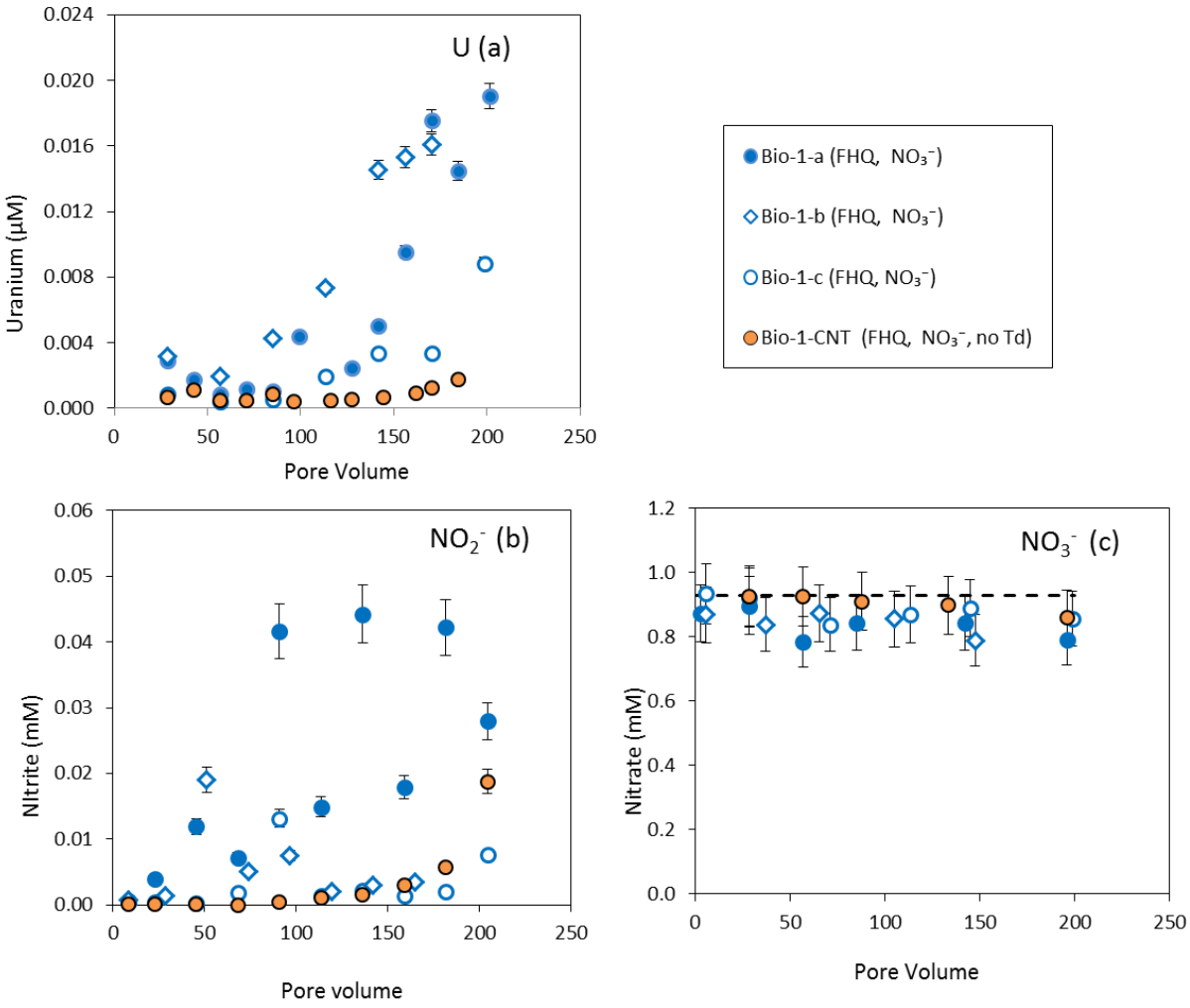

Figure 8. U(VI), NO_2^- and NO_3^- released from biotic and abiotic control columns reacted with 1 mM NO_3. Data points in color blue are triplicates and represents biotic experiment with *T. denitrificans*. Dashed line indicates input solution concentrations. FHQ in the index symbolizes column packed with ferrihydrite coated quartz. CNT represents control column with *T. denitrificans*. Dashed line is the measured input solution concentration.

4.5.3 Abiotic columns without Fe^{2+}

Higher total U release was seen in presence of NO_2^- as an oxidant (AB-2, AB-3-a and AB-3-b) than with NaCl (AB-1) (Figure. 9a). Steady state U release for the abiotic columns with 1 mM NO_2^- as input solution was obtained at around 200 pore volume. The

higher U released in presence of NO_2^- compared to a NaCl solution suggests that NO_2^- oxidize Bio-U(IV)$O_{2(s)}$ under anaerobic and abiotic conditions. A slight increase in U release at steady state was observed in columns packed with ferrihydrite (AB-3-a, AB-3-b) compared to the columns packed with quartz (AB-2). However the change was not that major. No significant differences were found for NO_2^- and NO_3^- concentrations for the columns at steady state and the slight variations were within the instrumental error range (Figure 9b).

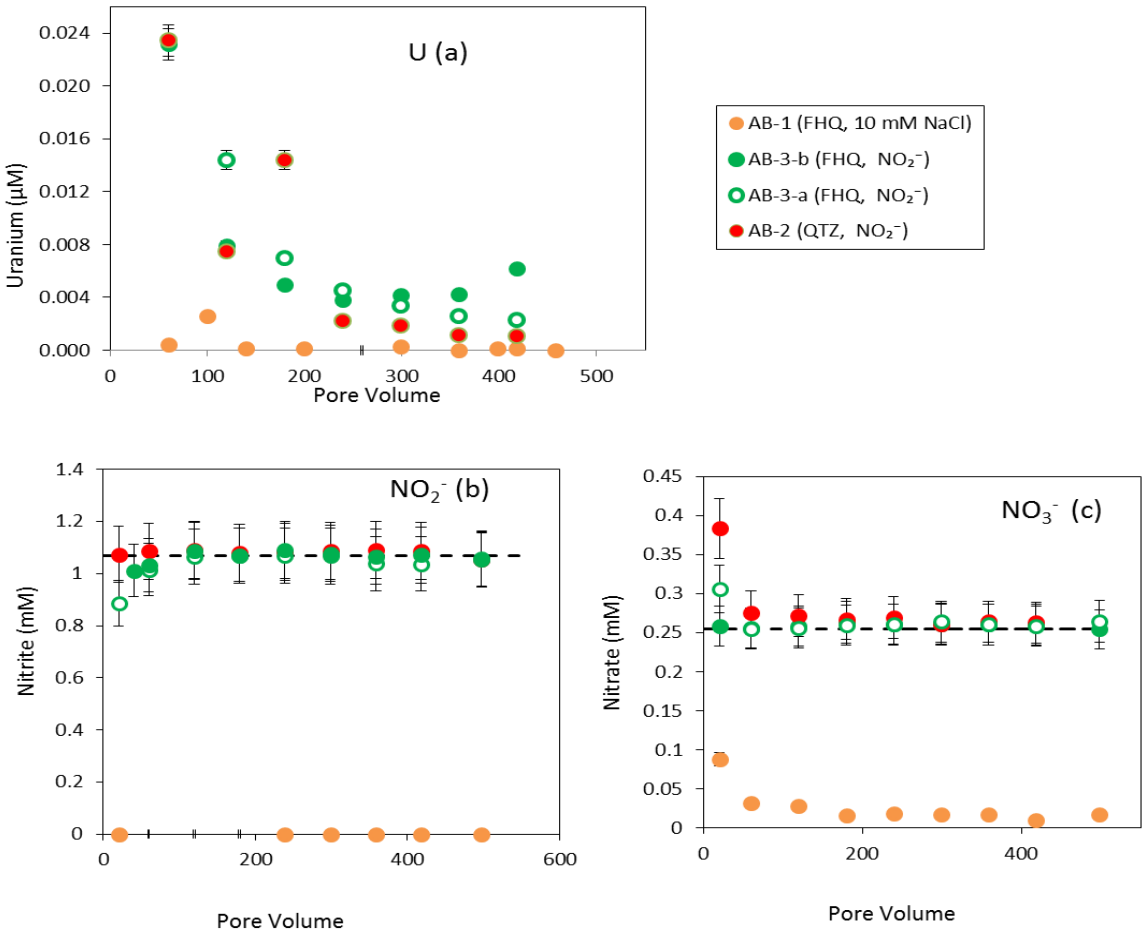

Figure 9: U(VI), NO_2^- and NO_3^- release from abiotic column experiment reacted with NO_2^-. Data points of the same color represent duplicates. Dashed line indicates input solution

concentrations. QTZ in the index symbolizes column packed with quartz. Dashed lines are the measured input solution concentration.

4.5.4 Biotic column with Fe^{2+}

In the presence of Fe^{2+}, release of U was higher in the abiotic column than in the columns with *T. denitrificans* during the first ~150 PV of reaction (Figure. 10a). This result is the opposite of what was observed in the system without Fe^{2+}. A slight increase in NO_2^- release was observed in the biotic columns packed with ferrihydrite-coated quartz (Bio-2-a, Bio-2-b) than the abiotic column (Bio-2-CNT) during the first ~150 PV (Figure. 10b). Nitrite concentrations for biotic columns packed with quartz were significantly higher but decreased with increasing pore volume. However, the change is less in comparison to the biotic columns without Fe^{2+}. The variations in NO_3^- , Fe^{2+} and Fe^{tot} release were within the error range of the input solution concentrations (Figure. 10c, 10d, 10e).

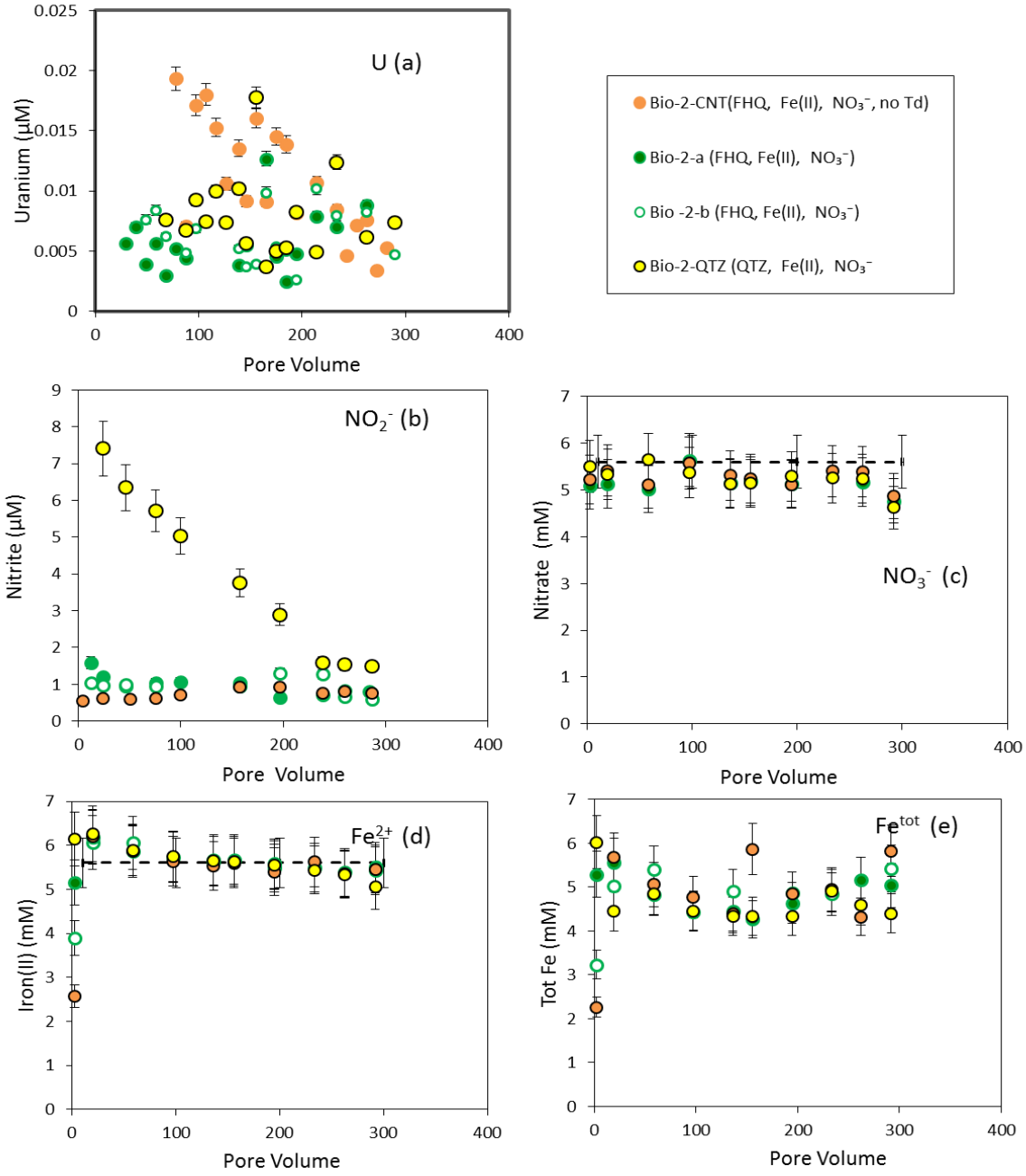

Figure 10: U(VI), NO_2^- , NO_3^- , Fe^{2+} and Fe^{tot} release from biotic column experiment reacted with 5 mM NO_3^- and 5 mM Fe^{2+}. Data points of the same color represent duplicates. Dashed lines are the measured input solution concentration

4.5.5 Abiotic columns with Fe^{2+}

In columns without *T. denitrificans*, total U release was found to be lowest when only Fe^{2+} was present in the input solution and highest when only NO_3^- was present in solution (Figure. 11a). Differences in U(VI) release were observed in columns packed with ferrihydrite-coated quartz and quartz (Figure. 11a). Higher concentrations of NO_2^- were released in column AB-10, which was packed with quartz and had both NO_3^- and Fe^{2+}in the input solution (Figure. 11b). Columns AB-9 and AB-11 had the lowest nitrite concentrations. No changes in Fe^{2+} concentration was observed in the effluent solution from columns with no NO_3^- in the input solution (Figure. 10c). However concentration of Fe^{2+} slightly decreased when NO_3^- was present (Figure 11c)

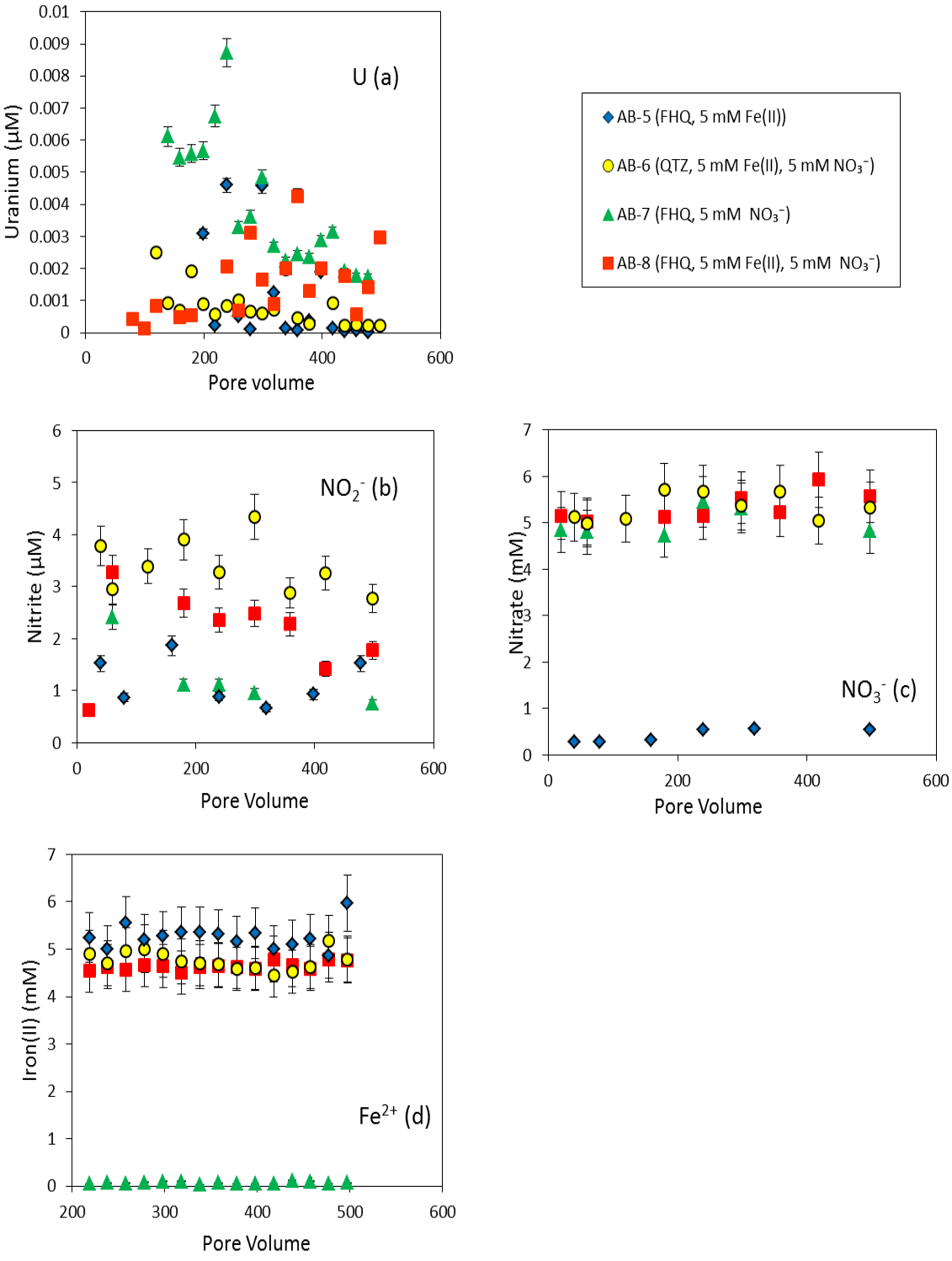

Figure 11: U(VI), NO_2^- , NO_3^- release from abiotic column experiment with soluble 5 mM Fe^{2+} and 5 mM NO_3^-. AB-7 is a control without Fe^{2+}. AB-5 is second experiment with NO_3^-. AB-6 is third control with quartz.

5. DISCUSSION

5.1 Structure of unreacted Bio-U(IV)$O_{2(s)}$ species

The particle size analysis of Bio-U(IV)$O_{2(s)}$ solids showed particles of different sizes in the same batch. The particle size analysis of Unr-1 calculated from surface area measurements by BET is ~7 nm, the value is similar to the one observed in the TEM images (4 nm). This range of particle size for Bio-U(IV)$O_{2(s)}$ has been reported in other studies as well (Burgos et al., 2008; Komlos et al., 2008; Renshaw et al., 2005; Senko et al., 2007; Singer et al., 2006; Singer et al., 2009) However the values are inconsistent with the DLS measurements done for Unr-2, which showed 2 populations of particles at 50 and 500 nm. This inconsistency can be due to aggregation of particles during the DLS measurements. The shape of lattice fringes observed in the TEM image of unreacted Bio-U(IV)$O_{2(s)}$ solids provided evidence that the Bio-U(IV)$O_{2(s)}$ solids are rounded nanocrystalline particles. Similar lattice fringes were also observed in the study conducted by Stewart Bd Fau - Girardot et al. (2012). Reduction in the amplitude of U-U backscattering for the unreacted Bio-U(IV)$O_{2(s)}$ relative to crystalline $UO_{2(s)}$ may be due to presence of non-uraninite species, small particle size of solids and poorly crystalline particles with high static disorder in the atomic structure (Asta et al., 2013 in prep; Bernier-Latmani et al., 2010; Senko et al., 2007; Sharp et al., 2011; Singer et al., 2006). However, reasons for the differences are still unclear. Prior studies have suggested that the difference is due of presence of ligands (like phosphoryl ligands), or slight variations in growth conditions during the bioreduction process (Bernier-Latmani et al., 2010;

Marshall et al., 2006; Senko et al., 2007). Both the differences in particle size and aggregation behavior of Bio-U(IV)$O_{2(s)}$ are likely to influence the oxidation process.

5.2 Oxidation experiments

All the biotic and abiotic flow-through column experiments conducted showed some amount of dissolution of Bio-U(IV)$O_{2(s)}$ in both presence or absence of oxidants. ICP-MS detection of uranium in all the effluent solution verified the dissolution of Bio-U(IV)$O_{2(s)}$ during the flow-through experiments. Table 2 and 3 shows differences in the mass of uranium in the column before and after the flow-through experiment. The results shows only partial dissolution of Bio-U(IV)$O_{2(s)}$ occurred in all biotic and abiotic columns. The results were similar to the one observed by Beller (2005), whose batch experiments showed only partial oxidation of Bio-U(IV)$O_{2(s)}$ in nitrate-dependent oxidation using *T. denitrificans*. The results are further verified by Senko et al. (2007), who showed incomplete Bio-U(IV)$O_{2(s)}$ oxidation under anaerobic conditions both in presence or absence of bacteria or oxidants. However there is inconsistency in the amount of dissolution between each column and some of the columns showed very low amount of uranium in the reacted sediments (AB-3-b, AB-6, Bio-1-a) indicating a very high dissolution. A possible explanation might be that the samples were inhomogeneous with uranium, while they were sampled for microwave digestion. Also the inhomogeneity can be a cause for higher amounts of uranium in some of the reacted biotic columns in Table 3.

It is evident from the experimental results that uranium redox state is significantly influenced by presence of NO_3^-, NO_2^-, Fe^{2+}, and Fe^{3+}. Nitrate and nitrite are

both able to oxidize Bio-U(IV)$O_{2(s)}$ (Figure. 8a and Figure. 9a). It is well known that Bio-U(IV)$O_{2(s)}$ oxidizes in presence of an electron acceptor (Beller, 2005; Senko et al., 2007). Both NO_3^- and NO_2^- accept electrons from Bio-U(IV)O_2 (s), oxidizing it to soluble U(VI), and producing reduced nitrogen species. Nitrate has a lower reduction potential than NO_2^- under anaerobic conditions (Estuardo et al., 2008), hence the thermodynamic drive to reduction to NO_2^- is low. However, the potential for reduction of NO_2 to NO^- is higher under anaerobic conditions, so it acts as a better electron acceptor and may oxidize more U(IV). In presence of *T. denitrificans*, higher concentrations of NO_2^- were released from columns from NO_3^- reduction, which released higher U concentrations than in abiotic control columns (Figure. 8b). Beller et al. (2006) verified c-type cytochromes present in the outer membrane of *T. denitrificans* have a high reduction potential and may serve as electron acceptors for U(IV) oxidation. Thus, with *T. denitrificans* present in the column as an electron acceptor, it may act as biotic pathway for Bio-U(IV)$O_{2(s)}$ oxidation, whereas NO_3^- and NO_2^- may act as an abiotic pathway. This combination of biotic and abiotic factor will complement each other thereby enhancing Bio-U(IV)$O_{2(s)}$ oxidation. Possible chemical reactions as well as the overall reaction proposed by Beller (2005) for nitrate-dependent oxidation of Bio-U(IV)$O_{2(s)}$ in presence of *T. denitrificans* is:

$$UO_2 \longrightarrow UO_2^{2+} + 2e^- \qquad (1) \qquad \text{Enzymatic biotic oxidation}$$

$$NO_3^- + 2e^- + 2H^+ \longrightarrow NO_2^- + H_2O \qquad (2) \qquad \text{Enzymatic subsequent reduction}$$

$$UO_2 \longrightarrow UO_2^{2+} + 2e^- \qquad (3) \qquad \text{Abiotic oxidation}$$

Overall reaction proposed by Beller (2005):

$$UO_2(s) + 0.4\,NO_3^- + 2.4\,H^+ \longrightarrow UO_2^{2+} + 0.2\,N_2 + 1.2\,H_2O \qquad (4)$$

Introduction of another electron donor, Fe^{2+}, affected the release of U from the columns. Both abiotic and biotic experiments showed that the presence of Fe^{2+} in the system significantly suppressed U release (Figure. 9a and 10a). Studies by Beller et al. (2013) have shown that the c-type cytochromes capable of nitrate-dependent oxidation of Bio-U(IV)$O_{2(s)}$ is different from the c-type cytochromes capable of nitrate-dependent Fe(II) oxidation both under anaerobic conditions. We hypothesize that *T. Denitrificans* favors oxidizing soluble Fe^{2+} instead of Bio-U(IV)$O_{2(s)}$. Highly sorptive ferric oxides may form from soluble Fe^{2+} oxidation which will sorb any U(VI) formed by oxidation by another c-type cytochromes. Electron transfer for Fe^{2+} oxidation may couple to NO_3^- reduction to NO_2^-. In the control flow-through experiment with no *T. denitrificans* higher amounts of U were released in the first 200 pore volume in comparison to the biotic columns (Figure. 10a). One possible hypothesis is that abiotic reduction of NO_3^- to NO_2^- is slow; hence its electron transfer coupling with soluble Fe^{2+} oxidation to form sorptive ferric oxide is also slow. Any U(VI) oxidized by electron coupling with NO_2^- reduction to NO^- is released in the effluent solution because the amount of ferric oxide for sorption is less. However in time as ferric oxide concentration increases with more Fe^{2+} oxidation, the subsequent release of U decreases. In systems with no oxidants, Fe^{2+} and Bio-U(IV)$O_{2(s)}$ are both electron donors and hence no redox changes occur (Figure. 11a). Plausible competing biotic and abiotic electron transfer mechanisms for system with *Thiobacillus denitrificans*, Bio-U(IV)$O_{2(s)}$, Fe^{2+} and NO_3^- system are shown below.

$2Fe^{2+} \rightarrow 2Fe^{3+} + 2e^-$ (5) Enzymatic biotic oxidation

$NO_3^- + 2e^- + 2H^+ \rightarrow NO_2^- + H_2O$ (6) Enzymatic subsequent reduction

$UO_2 \rightarrow UO_2^{2+} + 2e^-$ (7) Enzymatic biotic oxidation by another c-type cytochromes

6. IMPLICATION IN IN-SITU BIOREMEDIATION

This study was undertaken to understand geochemical mechanisms underlying the pathways for oxidation of Bio-U(IV)$O_{2(s)}$ in presence of *T. denitrificans*, NO_3^-, NO_2^-, Fe^{3+} and Fe^{2+}. Several other studies have been conducted on batch experiments previously explaining the oxidation of Bio-U(IV)$O_{2(s)}$. Although, these studies fail to separate key biotic and abiotic pathways associated. Our studies have shown changes in oxidation chemistry of Bio-U(IV)$O_{2(s)}$ in presence of iron in the system. Flow-through experiments conducted without the Fe(II) system have shown that presence of *T. denitrificans* with NO_3^- releases more U than without *T. denitrificans*. Plausible biotic and abiotic pathways for U release have been elucidated in our study. Another significant finding is the decrease in U release in presence of Fe^{2+}. Observing the results of flow-through experiment and EXAFS spectra, we hypothesized that T. denitrificans favours oxidizing soluble Fe^{2+} instead of Bio-U(IV)$O_{2(s)}$. The oxidized product is highly sorptive and therefore sorbs U(VI) oxidized by abiotic pathways. Spectroscopic data has verified

presence of U(VI) in both abiotic and biotic reacted columns in which soluble Fe^{2+} was passed. However more detailed analysis of unreacted and reacted Bio-U(IV)$O_{2(s)}$ should be done to understand accurately the structural changes during the oxidation process. Nevertheless our finding that the addition of an electron donor might slow down the oxidative dissolution of Bio-U(IV)$O_{2(s)}$ might contribute to developing an effective remediation strategy for contaminant uranium in the future.

REFERENCES

Asta, M.P., Kanematsu, M., Pokharel, R., Zhou, P., Beller, H., O'Day, P., 2013 in prep. Anaerobic oxidation of U(IV)-oxide by abiotic and nitrate-dependent bacterial pathways. Part II: Kinetic analysis and reactive transport modeling.

Beller, H.R., 2005. Anaerobic, nitrate-dependent oxidation of U (IV) oxide minerals by the chemolithoautotrophic bacterium Thiobacillus denitrificans. Applied and Environmental Microbiology 71, 2170-2174.

Beller, H.R., Chain, P.S., Letain, T.E., Chakicherla, A., Larimer, F.W., Richardson, P.M., Coleman, M.A., Wood, A.P., Kelly, D.P., 2006. The genome sequence of the obligately chemolithoautotrophic, facultatively anaerobic bacterium Thiobacillus denitrificans. Journal of bacteriology 188, 1473-1488.

Beller, H.R., Zhou, P., Legler, T.C., Chakicherla, A., Kane, S., Letain, T.E., O'Day, P.A., 2013. Genome-enabled studies of anaerobic, nitrate-dependent iron oxidation in the chemolithoautotrophic bacterium Thiobacillus denitrificans. Frontiers in Microbiology 4.

Bendschneider, K., Robinson, R.J., 1952. A new spectrophotometric method for the determination of nitrite in sea water: Journal of Marine Research, v. 11, p. 87-96.

Bernier-Latmani, R., Veeramani, H., Vecchia, E.D., Junier, P., Lezama-Pacheco, J.S., Suvorova, E.I., Sharp, J.O., Wigginton, N.S., Bargar, J.R., 2010. Non-uraninite products of microbial U(VI) reduction. Environmental science & technology 44, 9456-9462.

Burgos, W.D., McDonough, J.T., Senko, J.M., Zhang, G., Dohnalkova, A.C., Kelly, S.D., Gorby, Y., Kemner, K.M., 2008. Characterization of uraninite nanoparticles produced by Shewanella oneidensis MR-1. Geochimica et Cosmochimica Acta 72, 4901-4915.

Charbonneau, M., 2009. Current problems and recent advances of insitu bioremediation of uranium contaminated sites. MMG 445 Basic Biotechnology. 5, 13-15.

Cornell, R.M., Schwertmann, U., 1996. The iron oxides: structure, properties, reactions, occurrences and uses Weinhein, VCH, New York.

EPA, U.S., 2000. National Primary Drinking Water Regulations; Radionuclides; Final Rule. 2000, 40 CFR Parts 9, 141, and 142. Fed. Regist. 65: 76707-76753.

Estuardo, C., Martí, M.C., Huiliñir, C., Aspé Lillo, E., Roeckel von Bennewitz, M., 2008. Improvement of nitrate and nitrite reduction rates prediction. Electronic Journal of Biotechnology 11, 73-82.

Finneran, K.T., Housewright, M.E., Lovley, D.R., 2002. Multiple influences of nitrate on uranium solubility during bioremediation of uranium-contaminated subsurface sediments. Environ. Microbiol. 4, 510-516.

Fredrickson, J.K., Zachara, J.M., Kennedy, D.W., Duff, M.C., Gorby, Y.A., Li, S.M.W., Krupka, K.M., 2000. Reduction of U(VI) in goethite (alpha-FeOOH) suspensions by a dissimilatory metalreducing bacterium. Geochim. Cosmochim. Acta 64

3085-3013.

Ginder-Vogel, M., Criddle, C.S., Fendorf, S., 2006. Thermodynamic constraints on the oxidation of biogenic UO_2 by Fe(III) (hydr) oxides. Environ. Sci. Technol. 40, 3544-3550.

Goldman, E., Jacobs, R., 1961. Determination of Nitrates by Ultraviolet Absorption. Journal (American Water Works Association) 53, 187-191.

Komlos, J., Mishra, B., Lanzirotti, A., Myneni, S., Jaffé, P., 2008. Real–Time Speciation of Uranium during Active Bioremediation and Reoxidation. Journal of Environmental Engineering 134, 78-86.

Langmuir, D., 1978. Uranium solution-mineral equilibria at low temperatures with applications to sedimentary ore deposits. Geochimica et Cosmochimica Acta 42, 547-569.

Loan, M., Richmond, W.R., Parkinson, G.M., 2005. On the crystal growth of nanoscale schwertmannite. Journal of Crystal Growth 275, e1875-e1881.

Loveley, D., Lonergan, D., 1990. Anaerobic Oxidation of Toluene, Phenol, and p-Cresol by the Dissimilatory Iron-Reducing Organism, GS-15. Applied Environmental Microbiology 56, 1858-1864.

Lovley, D.R., Phillips, E.J.P., 1992a. Bioremediation of uranium contamination with enzymatic uranium reduction. Environ. Sci. Technol. 26, 2228-2234.

Lovley, D.R., Phillips, E.J.P., 1992b. Reduction of uranium by *Desulfovibrio-desulfuricans*. Appl. Environ. Microbiol. 58, 850-856.

Lovley, D.R., Phillips, E.J.P., Gorby, Y.A., Landa, E.R., 1991. Microbial reduction of uranium. Nature 350, 413-416.

Lovley, D.R., Widman, P.K., Woodward, J.C., Phillips, E.J.P., 1993. Reduction of uranium by cytochrome-C(3) of *Desulfovibrio-vulgaris*. Appl. Environ. Microbiol. 59, 3572-3576.

Marshall, M.J., Beliaev, A.S., Dohnalkova, A.C., Kennedy, D.W., Shi, L., Wang, Z., Boyanov, M.I., Lai, B., Kemner, K.M., McLean, J.S., Reed, S.B., Culley, D.E., Bailey, V.L., Simonson, C.J., Saffarini, D.A., Romine, M.F., Zachara, J.M., Fredrickson, J.K., 2006. c-Type cytochrome-dependent formation of U(IV) nanoparticles by Shewanella oneidensis. PLoS biology 4, e268.

Moon, E.M., Peacock, C.L., 2013. Modelling Cu(II) adsorption to ferrihydrite and ferrihydrite–bacteria composites: Deviation from additive adsorption in the composite sorption system. Geochimica et Cosmochimica Acta 104, 148-164.

Ravel, B., Newville, V., 2005. ATHENA, ARTEMIS, HEPHAESTUS: data analysis for X-ray absorption spectroscopy using IFEFFIT. J. Synchrotron Radiation 12: 537-541.

Renshaw, J.C., Butchins, L.J.C., Livens, F.R., May, I., Charnock, J.M., Lloyd, J.R., 2005. Bioreduction of Uranium: Environmental Implications of a Pentavalent Intermediate. Environmental Science & Technology 39, 5657-5660.

Sani, R.K., Peyton, B.M., Dohnalkova, A., Amonette, J.E., 2005a. Reoxidation of reduced uranium with iron(III) (hydr)oxides under sulfate-reducing conditions. Environmental science & technology 39, 2059-2066.

Sani, R.K., Peyton, B.M., Dohnalkova, A., Amonette, J.E., 2005b. Reoxidation of reduced uranium with iron(III) (hydr)oxides under sulfate-reducing conditions. Environ. Sci. Technol. 39, 2059-2066.

Schofield, E.J., Veeramani, H., Sharp, J.O., Suvorova, E., Bernier-Latmani, R., Mehta, A., Stahlman, J., Webb, S.M., Clark, D.L., Conradson, S.D., Ilton, E.S., Bargar, J.R., 2008. Structure of biogenic uraninite produced by Shewanella oneidensis strain MR-1. Environmental science & technology 42, 7898-7904.

Schwertmann, U., Cornell, R.M., 2007. Frontmatter, Iron Oxides in the Laboratory. Wiley-VCH Verlag GmbH, pp. i-xviii.

Senko, J.M., Istok, J.D., Suflita, J.M., Krumholz, L.R., 2002. In-situ evidence for uranium immobilization and remobilization. Environmental science & technology 36, 1491-1496.

Senko, J.M., Kelly, S.D., Dohnalkova, A.C., McDonough, J.T., Kemner, K.M., Burgos, W.D., 2007. The effect of U(VI) bioreduction kinetics on subsequent reoxidation of biogenic U(IV). Geochimica et Cosmochimica Acta 71, 4644-4654.

Senko, J.M., Mohamed, Y., Dewers, T.A., Krumholz, L.R., 2005a. Role for Fe(III) minerals in nitrate-dependent microbial U(IV) oxidation. Environ. Sci. Technol. 39, 2529-2536.

Senko, J.M., Suflita, J.M., Krumholz, L.R., 2005b. Geochemical controls on microbial nitrate-dependent U(IV) oxidation. Geomicrobiol. J. 22, 371-378.

Sharp, J.O., Lezama-Pacheco, J.S., Schofield, E.J., Junier, P., Ulrich, K.-U., Chinni, S., Veeramani, H., Margot-Roquier, C., Webb, S.M., Tebo, B.M., Giammar, D.E., Bargar, J.R., Bernier-Latmani, R., 2011. Uranium speciation and stability after reductive immobilization in aquifer sediments. Geochimica et Cosmochimica Acta 75, 6497-6510.

Singer, D.M., Farges, F., Brown, G.E., 2006. Biogenic UO2. Characterization and Surface Reactivity, 13th International Conference on X-Ray Absorption Fine Structure (XAFS13), November ed, pp. 3-5.

Singer, D.M., Farges, F.o., Brown, G.E., 2009. Biogenic nanoparticulate UO2: Synthesis, characterization, and factors affecting surface reactivity. Geochimica et Cosmochimica Acta 73, 3593-3611.

Stewart Bd Fau - Girardot, C., Girardot C Fau - Spycher, N., Spycher N Fau - Sani, R.K., Sani Rk Fau - Peyton, B.M., Peyton, B.M., 2012. Influence of chelating agents on biogenic uraninite reoxidation by Fe(III) (Hydr)oxides.

Tokunaga, T.K., Wan, J.M., Kim, Y.M., Sutton, S.R., Newville, M., Lanzirotti, A., Rao, W., 2008. Real-time X-ray absorption spectroscopy of uranium, iron, and manganese in contaminated sediments during bioreduction. Environ. Sci. Technol. 42, 2839-2844.

Ulrich, K.-U., Singh, A., Schofield, E.J., Bargar, J.R., Veeramani, H., Sharp, J.O., Bernier-Latmani, R., Giammar, D.E., 2008. Dissolution of biogenic and synthetic UO2 under varied reducing conditions. Environmental science & technology 42, 5600-5606.

Veeramani, H., Schofield, E.J., Sharp, J.O., Suvorova, E.I., Ulrich, K.-U., Mehta, A., Giammar, D.E., Bargar, J.R., Bernier-Latmanit, R., 2009. Effect of Mn(II) on the structure and reactivity of biogenic uraninite. Environmental science & technology 43, 6541-6547.

Viollier, E., Inglett, P.W., Hunter, K., Roychoudhury, A.N., Van Cappellen, P., 2000. The ferrozine method revisited: Fe(II)/Fe(III) determination in natural waters. Applied Geochemistry 15, 785-790.

Wan, J.M., Tokunaga, T.K., Brodie, E., Wang, Z.M., Zheng, Z.P., Herman, D., Hazen, T.C., Firestone, M.K., Sutton, S.R., 2005. Reoxidation of bioreduced uranium under reducing conditions. Environ. Sci. Technol. 39, 6162-6169.

Waychunas, G.A., 2001. Structure, Aggregation and Characterization of Nanoparticles. Reviews in Mineralogy and Geochemistry 44: 105-166.

Webb, S.M., 2005. Sixpack: A graphical user interface for XAS analysis using IFEFFIT. Phys. Scr., T115, 1011–1014.

Widdel, F., Bak, F., 1992. Gram-negative mesophilic sulfate-reducing bacteria, p. 3352-3378. In A. Balows, H. G. Trüper, M. Dworkin, W. Harder, and K.-H. Schleifer (ed.), The prokaryotes. Springer-Verlag, New York, N.Y.

APPENDIX

A1: Bromide tracer data for biotic and abiotic columns

Reacted Biotic Column		Reacted Abiotic Column	
Pore Volume	Br^- [ppm]	Pore Volume	Br^- [ppm]
0	0.61	0.00	Below detection
0.53	0.22	2.31	Below detection
1.06	Below detection	4.63	Below detection
1.60	0.93	6.94	0.12
2.13	6.34	9.26	0.47
2.66	13.97	11.57	0.76
3.19	21.24	13.89	0.91
3.72	27.29	16.20	0.98
4.26	31.35	18.52	1.02
4.79	34.36	20.83	1.04
5.32	36.44	23.15	0.92
5.85	37.81	25.46	0.42
6.38	38.90	27.78	0.21
6.91	39.84	30.09	0.12
7.45	38.43	32.41	0.08
7.98	29.83	34.72	0.05
8.51	17.69	37.04	0.04
9.04	9.77	39.35	0.03
9.57	5.70	41.67	0.02
10.11	3.44	43.98	0.01
10.64	2.06	46.30	Below detection
11.17	1.20		
11.70	0.60		
12.23	0.19		
12.77	Below detection		

A2: Effluent solution analysis for biotic columns without Fe^{2+}

Column	Time (min)	Pore Volume	U [uM]	$NO3^-$ [mM]	$NO2^-$			
Bio-1-CNT-4	320	11.3			Column	Time (min	Pore Volume	$NO2^-$ [mM]
Bio-1-CNT-10	800	28.4	0.00064	0.93	Bio-1-CNT-3	240	8.51	8.2213E-05
Bio-1-CNT-15	1200	42.6	0.00114		Bio-1-CNT-8	640	22.69	4.1107E-05
Bio-1-CNT-20	1600	56.7	0.00049	0.92	Bio-1-CNT-16	1280	45.39	7.1937E-05
Bio-1-CNT-25	2000	70.9	0.00045		Bio-1-CNT-24	1920	68.08	1.0277E-05
Bio-1-CNT-30	2400	85.1	0.00085	0.91	Bio-1-CNT-32	2560	90.78	4.3162E-04
Bio-1-CNT-34	2720	96.5	0.00043		Bio-1-CNT-40	3200	113.47	1.0688E-03
Bio-1-CNT-41	3280	116.3	0.00048		Bio-1-CNT-48	3840	136.17	1.6134E-03
Bio-1-CNT-45	3600	127.7	0.00052	0.9	Bio-1-CNT-56	4480	158.86	3.0676E-03
Bio-1-CNT-51	4080	144.7	0.00064		Bio-1-CNT-64	5120	181.56	5.7241E-03
Bio-1-CNT-57	4560	161.7	0.00091		Bio-1-CNT-72	5760	204.25	1.8745E-02
Bio-1-CNT-60	4800	170.2	0.00125					
Bio-1-CNT-65	5200	184.4	0.00176					
Bio-1-CNT-71	5680	201.4	0.00498	0.86				
Bio-1-a-1	80	2.8		0.87	Bio-1-a-3	240	8.51	5.0870E-04
Bio-1-a-5	400	14.2			Bio-1-a-8	640	22.69	3.9771E-03
Bio-1-a-10	800	28.4	0.00290	0.9	Bio-1-a-16	1280	45.39	1.1906E-02
Bio-1-a-15	1200	42.6	0.00174		Bio-1-a-24	1920	68.08	7.1885E-03
Bio-1-a-20	1600	56.7	0.00087	0.78	Bio-1-a-32	2560	90.78	4.1692E-02
Bio-1-a-25	2000	70.9	0.00115		Bio-1-a-40	3200	113.47	1.4932E-02
Bio-1-a-30	2400	85.1	0.00103	0.84	Bio-1-a-48	3840	136.17	4.4246E-02
Bio-1-a-35	2800	99.3	0.00441		Bio-1-a-56	4480	158.86	1.7887E-02
Bio-1-a-45	3600	127.7	0.00245		Bio-1-a-64	5120	181.56	4.2227E-02
Bio-1-a-50	4000	141.8	0.00502	0.84	Bio-1-a-72	5760	204.25	2.7958E-02

Bio-1-a-55	4400	156.0	0.00955					
Bio-1-a-60	4800	170.2	0.01753					
Bio-1-a-65	5200	184.4	0.01447					
Bio-1-a-71	5680	201.4	0.01905	0.79				
Bio-1-b-1	80	2.8		0.87	Bio-1-b-3	240	8.51	7.9644E-04
Bio-1-b-10	800	28.4	0.00315	0.84	Bio-1-b-10	800	28.36	1.4182E-03
Bio-1-b-20	1600	56.7	0.00198	0.87	Bio-1-b-18	1440	51.06	1.9032E-02
Bio-1-b-30	2400	85.1	0.00425		Bio-1-b-26	2080	73.75	5.1332E-03
Bio-1-b-40	3200	113.5	0.00732	0.86	Bio-1-b-34	2720	96.45	7.4711E-03
Bio-1-b-50	4000	141.8	0.01456	0.79	Bio-1-b-42	3360	119.14	2.0451E-03
Bio-1-b-55	4400	156.0	0.01531		Bio-1-b-50	4000	141.84	2.9391E-03
Bio-1-b-60	4800	170.2	0.01605		Bio-1-b-58	4640	164.53	3.4016E-03
Bio-1-c-1	80	2.8		0.93	Bio-1-c-3	240	8.51	4.9328E-04
Bio-1-c-10	800	28.4	0.00084	0.92	Bio-1-c-8	640	22.69	4.1107E-04
Bio-1-c-20	1600	56.7	0.00038	0.84	Bio-1-c-16	1280	45.39	2.7747E-04
Bio-1-c-30	2400	85.1	0.00053		Bio-1-c-32	2560	90.78	1.3144E-02
Bio-1-c-40	3200	113.5	0.00196	0.87	Bio-1-c-40	3200	113.47	1.3462E-03
Bio-1-c-50	4000	141.8	0.00333	0.89	Bio-1-c-48	3840	136.17	2.2506E-03
Bio-1-c-60	4800	170.2	0.00338		Bio-1-c-64	5120	181.56	2.0708E-03
Bio-1-c-70	5600	198.6	0.00883	0.86	Bio-1-c-72	5760	204.25	7.5585E-03

A3: Effluent solution analysis for abiotic columns without Fe^{2+}

Column	Time (min)	Pore Volume	U [uM]	$NO3^-$	$NO2^-$ [mM]
AB-1- 1	215	19.9	0.0004	0.0869	0.0003
AB-1- 3	645	59.72	0.0026	0.0317	-0.0001
AB-1- 6	1290	119.44	0.0002	0.0271	0.0000
AB-1- 9	1935	179.16	0.0002	0.0159	-0.0001
AB-1- 12	2580	238.88	0.0000	0.0172	0.0000
AB-1- 15	3225	298.61	0.0000	0.0169	0.0007
AB-1- 18	3870	358.33	0.0001	0.0167	0.0002
AB-1- 21	4515	418.05	0.0001	0.0098	0.0001
AB-1- 25	4945	457.87	0.0000	0.0161	
AB-2- 1	215	19.9		0.3832	1.0729
AB-2- 3	645	59.72	0.0234	0.2753	1.0852
AB-2- 6	1290	119.44	0.0075	0.2714	1.0914
AB-2- 9	1935	179.16	0.0144	0.2671	1.0791
AB-2- 12	2580	238.88	0.0022	0.2690	1.0832
AB-2- 15	3225	298.61	0.0018	0.2600	1.0873
AB-2- 18	3870	358.33	0.0011	0.2638	1.0914
AB-2- 21	4515	418.05	0.0011	0.2624	1.0873
AB-2- 25	5375	497.68	0.0012	0.2608	1.0523
AB-3-a- 1	215	19.9		0.3059	0.8858
AB-3-a- 3	645	59.72		0.2539	1.0153
AB-3-a- 6	1290	119.44	0.0144	0.2556	1.0647
AB-3-a- 9	1935	179.16	0.0070	0.2594	1.0688
AB-3-a- 12	2580	238.88	0.0045	0.2602	1.0688
AB-3-a- 15	3225	298.61	0.0034	0.2635	1.0770
AB-3-a- 18	3870	358.33	0.0026	0.2600	1.0379
AB-3-a- 21	4515	418.05	0.0023	0.2578	1.0359
AB-3-a- 25	5375	497.68	0.0082	0.2641	1.0585
AB-3-b- 2	430	39.81	0.1790	0.2578	1.0112
AB-3-b- 3	645	59.72	0.0231	0.2553	1.0318
AB-3-b- 6	1290	119.44	0.0079	0.2578	1.0873
AB-3-b- 9	1935	179.16	0.0049	0.2630	1.0688
AB-3-b- 12	2580	238.88	0.0038	0.2605	1.0914
AB-3-b- 15	3225	298.61	0.0042	0.2608	1.0667
AB-3-b- 18	3870	358.33	0.0042	0.2600	1.0647
AB-3-b- 21	4515	418.05	0.0062	0.2600	1.0708
AB-3-b- 25	5375	497.68	0.0135	0.2539	1.0544

A4: Effluent solution analysis for biotic columns with Fe^{2+}

Column	Time (min)	Pore Volume	U [uM]	NO_3^- [mM]	Fe(II) [mM]	Tot Fe [mM]	NO_2^-			
Bio-2-CNT-1	80	2.43161		5.22739	2.56941	2.25922	Column	Time (min)	Pore Volume	NO_2^- [uM]
Bio-2-CNT-4	320	9.72644					Bio-2-CNT-1	80	2.43161	0.53439
Bio-2-CNT-8	640	19.45289		5.41497	6.20085	5.67144	Bio-2-CNT-10	800	24.31611	0.61660
Bio-2-CNT-12	960	29.17933					Bio-2-CNT-21	1680	51.06383	0.59091
Bio-2-CNT-16	1280	38.90578					Bio-2-CNT-31	2480	75.37994	0.61660
Bio-2-CNT-20	1600	48.63222					Bio-2-CNT-41	3280	99.69605	0.71423
Bio-2-CNT-24	1920	58.35866		5.11442	5.85762	5.06134	Bio-2-CNT-65	5200	158.05471	0.91462
Bio-2-CNT-28	2240	68.08511					Bio-2-CNT-81	6480	196.96049	0.92490
Bio-2-CNT-32	2560	77.81155	0.01935				Bio-2-CNT-98	7840	238.29787	0.74506
Bio-2-CNT-36	2880	87.53799	0.00707				Bio-2-CNT-107	8560	260.18237	0.80672
Bio-2-CNT-40	3200	97.26444	0.01713	5.57722	5.63051	4.76353	Bio-2-CNT-118	9440	286.93009	0.74506
Bio-2-CNT-44	3520	106.99088	0.01801							
Bio-2-CNT-48	3840	116.71733	0.01528							
Bio-2-CNT-52	4160	126.44377	0.01061	5.30822	5.53413	4.39059				
Bio-2-CNT-57	4560	138.60182	0.01354							
Bio-2-CNT-60	4800	145.89666	0.00917							
Bio-2-	5120	155.623	0.0160	5.2413	5.5952	5.8649				

CNT-64		10	2	6	9	4				
Bio-2-CNT-68	5440	165.34954	0.00911							
Bio-2-CNT-72	5760	175.07599	0.01453							
Bio-2-CNT-76	6080	184.80243	0.01389							
Bio-2-CNT-80	6400	194.52888	0.00815	5.11667	5.39842	4.85284				
Bio-2-CNT-88	7040	213.98176	0.01068							
Bio-2-CNT-92	7360	223.70821								
Bio-2-CNT-96	7680	233.43465	0.00845	5.39852	5.62815	4.95389				
Bio-2-CNT-100	8000	243.16109	0.00467							
Bio-2-CNT-104	8320	252.88754	0.00714							
Bio-2-CNT-108	8640	262.61398	0.00761	5.38411	5.35893	4.32248				
Bio-2-CNT-112	8960	272.34043	0.00340							
Bio-2-CNT-116	9280	282.06687	0.00532							
Bio-2-CNT-119	9520	289.36170		4.87013	5.45622	5.82243				
Bio-2-a-1	80	2.43161		5.09290	5.14894	5.28677	Bio-2-a-5	400	12.15805	1.03794
Bio-2-a-4	320	9.72644					Bio-2-a-10	800	24.31611	0.97115
Bio-2-a-8	640	19.45289		5.13022	6.17908	5.55031	Bio-2-a-19	1520	46.20061	0.98656
Bio-2-a-12	960	29.17933	0.00566				Bio-2-a-31	2480	75.37994	0.93518
Bio-2-a-16	1280	38.90578	0.00704				Bio-2-a-65	5200	158.05471	0.95573
Bio-2-a-20	1600	48.63222	0.00394				Bio-2-a-81	6480	196.96049	1.30000

Bio-2-a-24	1920	58.35866	0.00563	5.02453	5.86345	4.83554	Bio-2-a-98	7840	238.29787	1.26403
Bio-2-a-28	2240	68.08511	0.00295				Bio-2-a-107	8560	260.18237	0.66798
Bio-2-a-32	2560	77.81155	0.00522				Bio-2-a-118	9440	286.93009	0.59605
Bio-2-a-36	2880	87.53799	0.00445							
Bio-2-a-40	3200	97.26444		5.63891	5.72465	4.43787				
Bio-2-a-44	3520	106.99088								
Bio-2-a-48	3840	116.71733								
Bio-2-a-52	4160	126.44377								
Bio-2-a-57	4560	138.60182	0.00386	5.14981	5.63284	4.44547				
Bio-2-a-60	4800	145.89666	0.00548							
Bio-2-a-64	5120	155.62310		5.19278	5.67799	4.26435				
Bio-2-a-68	5440	165.34954	0.01268							
Bio-2-a-72	5760	175.07599	0.00455							
Bio-2-a-76	6080	184.80243	0.00247							
Bio-2-a-80	6400	194.52888	0.00481	5.13420	5.58235	4.63130				
Bio-2-a-88	7040	213.98176	0.00791							
Bio-2-a-92	7360	223.70821								
Bio-2-a-96	7680	233.43465	0.00705							
Bio-2-a-100	8000	243.16109								
Bio-2-a-104	8320	252.88754								
Bio-2-a-108	8640	262.61398	0.00882	5.16919	5.38554	5.16389				
Bio-2-a-112	8960	272.34043								
Bio-2-a-116	9280	282.06687								
Bio-2-a-119	9520	289.36170		4.76489	5.51254	5.04368				
Bio-2-b-1	80	2.43161		4.73502	3.89264	3.23181	B36-5	400	12.15805	1.57747
Bio-2-b-4	320	9.72644					B36-10	800	24.31611	1.19209
Bio-2-	640	19.4528		5.7179	6.0619	5.0202	B36-	1520	46.2006	0.9557

b-8		9		5	0	1	19		1	3
Bio-2-b-12	960	29.17933					B36-31	2480	75.37994	1.04822
Bio-2-b-16	1280	38.90578					B36-41	3280	99.69605	1.07391
Bio-2-b-20	1600	48.63222	0.00762				B36-65	5200	158.05471	1.04822
Bio-2-b-24	1920	58.35866	0.00837	4.82798	6.05365	5.39439	B36-81	6480	196.96049	0.62688
Bio-2-b-28	2240	68.08511	0.00622				B36-98	7840	238.29787	0.70395
Bio-2-b-32	2560	77.81155					B36-107	8560	260.18237	0.82727
Bio-2-b-36	2880	87.53799	0.00486				B36-117	9360	284.49848	0.80672
Bio-2-b-40	3200	97.26444	0.00687							
Bio-2-b-44	3520	106.99088								
Bio-2-b-48	3840	116.71733								
Bio-2-b-52	4160	126.44377								
Bio-2-b-57	4560	138.60182	0.00523	5.92598	5.66503	4.90323				
Bio-2-b-60	4800	145.89666	0.00370							
Bio-2-b-64	5120	155.62310	0.00392							
Bio-2-b-68	5440	165.34954	0.00985							
Bio-2-b-72	5760	175.07599	0.00533							
Bio-2-b-76	6080	184.80243	0.00499							
Bio-2-b-80	6400	194.52888	0.00263	5.62747	5.48260	4.86012				
Bio-2-b-88	7040	213.98176	0.01016							
Bio-2-b-92	7360	223.70821								
Bio-2-b-96	7680	233.43465	0.00794	5.73867	5.48905	4.84018				
Bio-2-b-100	8000	243.16109								
Bio-2-b-104	8320	252.88754								
Bio-2-b-108	8640	262.61398	0.00827							
Bio-2-b-112	8960	272.34043								
Bio-2-b-116	9280	282.06687								

Bio-2-b-119	9520	289.36170	0.00474	5.38098	5.42645	5.41910				

A5: Effluent solution analysis for abiotic columns with Fe^{2+}

Column	Time (min)	Pore Volume	U [uM]	$NO3^-$ [mM]	$NO2^-$ [µM]	Fe(II) [mM]
AB5-1	215	19.90741				
AB5-2	430	39.81481		0.27326	1.52609	
AB5-3	645	59.72222				
AB5-4	860	79.62963		0.27956	0.86667	
AB5-5	1075	99.53704				
AB5-6	1290	119.44444				
AB5-7	1505	139.35185				
AB5-8	1720	159.25926		0.32783	1.86522	
AB5-9	1935	179.16667				
AB5-10	2150	199.07407	0.00308			
AB5-11	2365	218.98148	0.00023			5.24545
AB5-12	2580	238.88889	0.00459	0.54254	0.88551	4.99930
AB5-13	2795	258.79630	0.00051			5.55588
AB5-14	3010	278.70370	0.00010			5.20339
AB5-15	3225	298.61111	0.00457			5.26809
AB5-16	3440	318.51852	0.00123	0.56115	0.65942	5.35490
AB5-17	3655	338.42593	0.00012			5.35424
AB5-18	3870	358.33333	0.00008			5.30945
AB5-19	4085	378.24074	0.00036			5.16670
AB5-20	4300	398.14815	0.00189		0.92319	5.34496
AB5-21	4515	418.05556	0.00012			5.00401
AB5-22	4730	437.96296	0.00003			5.10098
AB5-23	4945	457.87037	0.00008			5.21256
AB5-24	5160	477.77778	0.00002			4.86726
AB5-25	5375	497.68519		0.55000	1.52609	5.96402
AB6-1	215	19.90741				
AB6-2	430	39.81481		5.12089	3.78696	
AB6-3	645	59.72222		4.98333	2.95797	
AB6-4	860	79.62963				
AB6-5	1075	99.53704				
AB6-6	1290	119.44444	0.00249	5.09002	3.39130	
AB6-7	1505	139.35185	0.00093			

AB6-8	1720	159.25926	0.00070			
AB6-9	1935	179.16667	0.00193	5.70395	3.90000	
AB6-10	2150	199.07407	0.00090			
AB6-11	2365	218.98148	0.00057			4.90761
AB6-12	2580	238.88889	0.00084	5.66493	3.27826	4.70108
AB6-13	2795	258.79630	0.00101			4.96618
AB6-14	3010	278.70370	0.00065			5.00837
AB6-15	3225	298.61111	0.00059	5.37260	4.33333	4.89804
AB6-16	3440	318.51852	0.00073			4.73752
AB6-17	3655	338.42593	0.00198			4.70616
AB6-18	3870	358.33333	0.00046	5.66484	2.88261	4.67990
AB6-19	4085	378.24074	0.00027			4.57962
AB6-20	4300	398.14815				4.60696
AB6-21	4515	418.05556	0.00093	5.04970	3.25942	4.44046
AB6-22	4730	437.96296	0.00023			4.52221
AB6-23	4945	457.87037	0.00024			4.62944
AB6-24	5160	477.77778	0.00021			5.18559
AB6-25	5375	497.68519	0.00023	5.33458	2.76957	4.79001
AB7-1	215	19.90741		4.84083		
AB7-2	430	39.81481				
AB7-3	645	59.72222		4.79606	2.41159	
AB7-4	860	79.62963				
AB7-5	1075	99.53704				
AB7-6	1290	119.44444				
AB7-7	1505	139.35185	0.00611			
AB7-8	1720	159.25926	0.00546			
AB7-9	1935	179.16667	0.00557	4.72443	1.11159	
AB7-10	2150	199.07407	0.00567			
AB7-11	2365	218.98148	0.00674			0.04825
AB7-12	2580	238.88889	0.00872	5.45197	1.11159	0.06511
AB7-13	2795	258.79630	0.00330			0.06292
AB7-14	3010	278.70370	0.00362			0.08244
AB7-15	3225	298.61111	0.00483	5.31371	0.94203	0.10390
AB7-16	3440	318.51852	0.00269			0.09685
AB7-17	3655	338.42593	0.00224			0.03885
AB7-18	3870	358.33333	0.00245			0.06865
AB7-19	4085	378.24074	0.00235			0.05630
AB7-20	4300	398.14815	0.00288			0.04625
AB7-21	4515	418.05556	0.00314			0.05836
AB7-22	4730	437.96296	0.00191			0.11965

AB7-23	4945	457.87037	0.00178			0.10258
AB7-24	5160	477.77778	0.00173			0.05805
AB7-25	5375	497.68519		4.81959	0.75362	0.06704
AB8-1	215	19.90741		5.15143	0.62174	
AB8-2	430	39.81481				
AB8-3	645	59.72222		5.02868	3.27826	
AB8-4	860	79.62963	0.00042			
AB8-5	1075	99.53704	0.00014			
AB8-6	1290	119.44444	0.00084			
AB8-7	1505	139.35185				
AB8-8	1720	159.25926	0.00050			
AB8-9	1935	179.16667	0.00055	5.13244	2.67536	
AB8-10	2150	199.07407				
AB8-11	2365	218.98148				4.53833
AB8-12	2580	238.88889	0.00206	5.15045	2.35507	4.62894
AB8-13	2795	258.79630	0.00070			4.57196
AB8-14	3010	278.70370	0.00312			4.67058
AB8-15	3225	298.61111	0.00165	5.53998	2.48696	4.64493
AB8-16	3440	318.51852	0.00090			4.51065
AB8-17	3655	338.42593	0.00199			4.63162
AB8-18	3870	358.33333	0.00427	5.21949	2.27971	4.64522
AB8-19	4085	378.24074	0.00130			4.63428
AB8-20	4300	398.14815	0.00201			4.57973
AB8-21	4515	418.05556		5.92615	1.41304	4.79047
AB8-22	4730	437.96296	0.00178			4.66711
AB8-23	4945	457.87037	0.00058			4.59416
AB8-24	5160	477.77778	0.00141			4.78128
AB8-25	5375	497.68519	0.00296	5.56962	1.77101	4.76690